Attrition Resistant Iron-Based Catalysts For F-T SBCRs

Final Report

Work Performed Under
Grant No. DE-FG26-01NT41360

for

U.S. Department of Energy
National Energy Technology Laboratory
Pittsburgh, PA 15236

by

Dr. Adeyinka A. Adeyiga
Department of Chemical Engineering
Hampton University
Hampton, VA 23668

April 2006

DISCLAIMER

This report was prepared as an account of work sponsored by an agency of the United States Government. Neither the United States Government nor any agency thereof, nor any of their employees, makes any warranty, express or implied, or assumes any legal liability or responsibility for the accuracy, completeness, or usefulness of any information, apparatus, product, or process disclosed, or represents that its use would not infringe privately owned rights. Reference herein to any specific commercial product, process, or service by trade name, trademark, manufacturer, or otherwise, does not necessarily constitute or imply its endorsement, recommendation, or favoring by the United States Government or any agency thereof. The views and opinions of authors expressed herein do not necessarily state or reflect those of the United States Government or any agency thereof.

ABSTRACT

The Fischer-Tropsch (F-T) reaction provides a way of converting coal-derived synthesis gas (CO+ H_2) to liquid fuels. Since the reaction is highly exothermic, one of the major problems in control of the reaction is heat removal. Recent work has shown that the use of slurry bubble column reactors (SBCRs) can largely solve this problem. The use of iron- (FE) based catalysts is attractive not only due to their low cost and ready availability, but also due to their high water-*gas shift* activity which makes it possible to use these catalysts with low H_2/CO ratios. However, a serious problem with the use of Fe catalysts in a SBCR is their tendency to undergo attrition. This can cause fouling/plugging of downstream filters and equipment; makes the separation of catalyst from the oil/wax product very difficult, if not impossible; and results in a steady loss of catalyst from the reactor.

Under a previous Department of Energy (DOE)/University Research Grant (UCR) grant, Hampton University reported, for the first time, the development of demonstrably attrition-resistant Fe F-T synthesis catalysts having good activity, selectivity, and attrition resistance. These catalysts were prepared by spray drying Fe catalysts with potassium (K), copper (Cu), and silica (SiO_2) as promoters. SiO_2 *was also used as a binder* for spray drying. These catalysts were tested for activity and selectivity in a laboratory-scale fixed-bed reactor. Fundamental understanding of attrition is being addressed by incorporating suitable binders into the catalyst recipe. This has resulted in the preparation of a *spray dried HPR-43* catalyst having average particle size (aps) of 70 μm with high attrition resistance. This HPR-43 attrition resistant, active and selective catalyst gave 95% CO conversion through 125 hours of testing in a fixed-bed at 270^{o}C, 1.48 MPa, H_2/CO=0.67

and 2.0 NL/g-cat/h with C_{5+} selectivity of >78% and methane selectivity of less than 5% at an α of 0.9.

Research is proposed to enable further development and optimization of these catalysts by (1) better understanding the role and interrelationship of various catalyst composition and preparation parameters on attrition resistance, activity, and selectivity of these catalysts, (2) the presence of sulfide ions on a precipitated iron catalyst, and (3) the effect of water on sulfided iron F-T catalysts for its activity, selectivity, and attrition. Catalyst preparations will be based on spray drying. The research employed, among other measurements, attrition testing and F-T synthesis at high pressure. Catalyst activity and selectivity is evaluated using a small fixed-bed reactor and a continuous stirred tank reactor (CSTR).

The catalysts were prepared by co-precipitation, followed by binder addition and spray drying at 250^{o}C in a 1-m-diameter, 2-m-tall spray dryer. The binder silica content was varied from 0 to 20 wt %.

The results show that the use of small amounts of precipitated SiO_2 alone in spray-dried Fe catalysts can result in good attrition resistance. All catalysts investigated with SiO_2 wt% $\leq$ 12 produced fines less than 10 wt% during the jet cup attrition test, making them suitable for long-term use in a slurry bubble column reactor. Thus, concentration rather than the type of SiO_2 incorporated into catalyst has a more critical impact on catalyst attrition resistance of spray-dried Fe catalysts. Lower amounts of SiO_2 added to a catalyst give higher particle densities and therefore higher attrition resistances. In order to produce a suitable SBCR catalyst, however, the amount of SiO_2 added has to be optimized to provide adequate surface area, particle density, and attrition resistance.

Two of the catalysts with precipitated and binder silica were tested in Texas A&M University's CSTR (Autoclave Engineers). The two catalysts were also tested at The Center for Applied Energy Research in Lexington, Kentucky of the University of Kentucky.

Spray-dried catalysts with compositions 100 Fe/5 Cu/4.2 K/11 (P) SiO_2 and 100 Fe/5 Cu/4.2 K/1.1 (B) SiO_2 have excellent selectivity characteristics (low methane and high C_{5+} yields), but their productivity and stability (deactivation rate) need to be improved. Mechanical integrity (attrition strength) of these two catalysts was markedly dependent upon their morphological features. The attrition strength of the catalyst made out of largely spherical particles (1.1 (B) SiO_2) was considerably higher than that of the catalyst consisting of irregularly shaped particles (11 (P) SiO_2).

ACKNOWLEDGEMENTS

This study was sponsored by the U.S. Department of Energy (DOE) under Grant No. DE-FG-26-01NT41360. The authors would like to acknowledge with gratitude the guidance provided by the DOE Contracting Officer's Representatives, Drs. Udaya Rao, Shelby Rogers, Benjamin C. B. Hsieh and Robert M. Kornosky. The authors also acknowledge the guidance of Süd-Chemie Inc.

Appreciation is also extended to the following people for their guidance and support: Dr. James Goodwin of Clemson University, Dr. Drago Bukur of Texas A&M University, Dr. Burt Davis of the University of Kentucky, and Dr. K. Jothimurugesan of Conoco Phillips Company, Ponca City, Oklahoma.

TABLE OF CONTENTS

List of Figures

List of Figures (Contd.)

List of Tables

NOMENCLATURE

(P)	Precipitated
(B)	Binder
CAER	Center of Advanced Energy Research
NETL	National Energy Technology Laboratory
SBCR	Slurry Bubble Column Reactor
WGS	Water Gas Shift
XRD	X-Ray Powder Diffraction
TPR	Temperature Programmed Reduction
SEM	Scanning Electron Microscope
EDXS	Energy Dispersive X-Ray Spectroscopy
PSD	Particle Size Distribution
FTS	Fischer-Tropsch Synthesis
TOS	Time on Stream
STSR	Stirred Tank Reactor

ATTRITION RESISTANT IRON-BASED FISCHER-TROPSCH CATALYSTS FOR F-T SBCRS

1.0 INTRODUCTION

Fischer-Tropsch Synthesis (FTS) is the reaction of carbon monoxide (CO) and hydrogen (H_2) (syngas) to form a wide variety of hydrocarbons, typically using iron- or cobalt-based catalysts. Currently there are two commercial FTS plants: SASTECH produces synthetic fuels and chemicals from coal (including recent expansions), and Shell is using FTS to convert natural gas to high value products in Malaysia. There are other units in the planning or construction stage: China plans to make town gas via FTS; Williams Company is constructing a pilot plant to determine the economics of underground coal gasification; and Exxon-Mobile is evaluating the possibility of locating a large natural gas-based FTS plant in Quatar. These activities clearly show that improvements and innovations in FTS are underway. This process is also strategically important to the United State because of its vast coal reserves, and because FTS represents the best means to make high quality transportation fuels and liquid products from coal. In addition to other technical challenges, one of the major problems in control of the reaction is heat removal. Recent progress in this area has focused on the use of a slurry bubble column reactor (SBCR). These reactors offer simple designs and low costs while still permitting high catalyst and reactor productivity. It is generally thought that this will be the reactor of choice for commercial, coal-based FTS in the United States.

Since modern coal gasification plants produce a syngas that is relatively lean in H_2 (H_2/CO = 0.5-0.7), a catalyst that is active for the FTS reaction ($CO + 2H_2 \rightarrow -CH_2- + H_2O$) and the water-gas shift (WGS) reaction ($CO + H_2O \rightarrow CO_2 + H_2$) is required. The overall reaction on these catalysts is thus $2CO + H_2 \rightarrow -CH_2- + CO_2$. This allows the efficient use of low H_2/CO syngas. Iron-based catalysts, which are active shift catalysts, are thus preferred over cobalt-based catalysts, which are not. Iron (Fe) is also much less expensive than cobalt.

Fischer-Tropsch (F-T) products are very desirable from an environmental point of view. Because F-T catalysts are very sulfur sensitive, the feed must be completely sulfur free, which means that the product is also sulfur free. In addition to being sulfur free, the product is also

nitrogen and aromatics free. F-T diesel fuel has a very high cetane number. Although raw F-T naphtha has a low octane number, it can be processed into high quality gasoline. F-T distillate also makes an excellent ethylene plant feedstock.

Catalyst development activities have involved an extensive effort to improve the performance of (Fe) catalysts. Iron catalyst development work has been carried out by the Center for Advanced Energy Research (CAER) and the National Energy Technology Laboratory's (NETL) Office of Science and Engineering Research (OSER). These efforts have resulted in the development of iron catalysts with much higher activities than previous catalysts. A problem with iron catalysts is that they tend to have low structural strength that with attrition tends to produce very small catalyst particles during slurry operations. This attrition causes plugging, fouling, difficulty in separating the catalyst from the wax product, and loss of the catalyst. This is due to the low attrition resistance of the Fe catalyst and the significant breakage of the Fe particles. Fe catalysts are subject to both chemical as well as physical attrition in a SBCR. Chemical attrition can be caused due to phase changes that any Fe catalyst goes through ($Fe_2O_3 \rightarrow Fe_3O_4 \rightarrow FeO \rightarrow Fe \rightarrow$ Fe carbides) potentially causing internal stresses within the particle and resulting in weakening, spalling or cracking. Physical attrition can result due to collisions between catalyst particles and with reactor wall. Catalyst particles of irregular shapes and non-uniform sizes produces by conventional methods are subject to greater physical attrition.

Another inherent complication associated with the iron-based catalyst is the catalyst pretreatment. Before synthesis, a catalyst precursor is pretreated to convert the catalyst into an active form. The pretreatment of Fe is not as straight forward as that for Ru, Co or Ni. Although pretreatment includes reduction of the iron particles, other processes are also involved. The pretreatment of iron F-T catalysts is not clearly understood. Part of the confusion stems from the fact that the nature and composition of iron catalysts change during reaction. These changes depend on the temperature, time of exposure to the reactant feed, nature of the reactor system, composition of the feed, and activation conditions (time and temperature). The common pretreatment conditions employed in the case of iron catalysts are H_2 reduction, CO reduction (and carbiding), or reduction in the reactant syngas. Work at the NETL has focused on the effect of catalyst pretreatment and the impact of the liquid starting medium on syngas conversion in a stirred tank slurry reactor.

Several phases of iron are known to exist when iron-based catalysts are subjected to F-T synthesis conditions. These include metallic iron (α -Fe), iron oxides (hematite, α-Fe_2O_3; magnetite, Fe_3O_4 and Fe_xO), and iron carbides, of which at least five different forms are known to exist. These include O-carbides (carbides with carbon atoms in octahedral interstices, ε-Fe_2C, ε'-$Fe_{2.2}C$, and Fe_xC) and TP-carbides (carbides with carbon atoms in trigonal prismatic interstices, χ -$Fe_{2.5}C$ and Fe_3C). The formation and distribution of these phases depend on the reaction conditions, reaction times, and state of the catalyst (reduced/unreduced, supported/unsupported, etc.). However, the role of each of these phases during the reaction has not been resolved.

Potassium and copper are typically used as chemical promoters for iron F-T catalysts. The adsorption of CO on iron results in a net withdrawal of electrons from the metal, whereas hydrogen adsorption tends to donate electrons to the metal. Potassium and the associated O^{2-} donate electrons to the metal, enhancing CO adsorption while weakening H_2 adsorption. This leads to decreased hydrogenation and increased chain growth during the synthesis reaction, yielding higher molecular weight products (i.e., a higher α). Lower olefins are also produced. Potassium also decreased methane (CH_4) production and increases WGS activity. Copper on the other hand is introduced to facilitate reduction of the iron itself. Copper is more effective in increasing the FTS reaction rate than potassium. Also the average molecular weight is increased in the presence of copper.

The objective of this research is to develop robust iron-based Fischer-Tropsch catalysts that have suitable activity, selectivity, and stability to be used in the slurry bubble column reactor. Specifically we aim to develop to: (i) improve the performance and preparation procedure of the high activity, high attrition resistant, high alpha iron-based catalysts synthesized at Hampton University, (ii) seek improvements in the catalyst performance through variations in process conditions, pretreatment procedures, and/or modification in catalyst preparation steps, and (iii) investigate the performance in a slurry reactor.

2.0 EXECUTIVE SUMMARY

Fischer-Tropsch (F-T) synthesis to convert syngas ($CO + H_2$) derived from natural gas or coal to liquid fuels and wax is a well-established technology. For low H_2 to CO ratio syngas produced from CO_2 reforming of natural gas or from gasification of coal, the use of Fe catalysts is attractive because of their high water gas shift activity in addition to their high F-T activity. Fe catalysts are also attractive due to their low cost and low methane selectivity. Because of the highly exothermic nature of the F-T reaction, there has been a recent move away from fixed-bed reactors toward the development of slurry bubble column reactors (SBCRs) that employ 30 to 90 μm catalyst particles suspended in a waxy liquid for efficient heat removal. However, the use of Fe F-T catalysts in an SBCR has been problematic due to severe catalyst attrition resulting in fines that plug the filter employed to separate the catalyst from the waxy product. Fe catalysts can undergo attrition in SBCRs not only due to vigorous movement and collisions but also due to phase changes that occur during activation and reaction.

The objectives of this research were to develop a better understanding of the parameters affecting attrition of Fe F-T catalysts suitable for use in SBCRs and to incorporate this understanding into the design of novel Fe catalysts having superior attrition resistance.

The catalysts were prepared by co-precipitation, followed by binder addition and spray drying at 250°C in a 1-m-diameter, 2-m-tall spray dryer. The binder silica content was varied from 0 to 20 wt %.

The results show that use of small amounts of precipitated silica (SiO_2) alone in spray-dried Fe catalysts can result in good attrition resistance. All catalysts investigated with SiO_2 wt% $\leq$ 12 produced fines less than 10 wt% during the jet cup attrition test, making them suitable for long-term use in a slurry bubble column reactor (SBCR). Thus, concentration rather than type of SiO_2 (precipitated or binder) incorporated into catalyst has a more critical impact on catalyst attrition resistance of spray-dried Fe catalysts. Lower amounts of SiO_2 added to a catalyst give higher particle densities and therefore higher attrition resistances. In order to produce a suitable SBCR catalyst, however, the amount of SiO_2 added has to be optimized to provide adequate surface area, particle density, and attrition resistance.

Two of the catalysts with precipitated and binder silica were tested in Texas A&M University's CSTR (Autoclave Engineers) and The Center for Applied Energy Research in Lexington, Kentucky of the University of Kentucky.

Spray-dried catalysts with compositions 100 Fe/5 Cu/4.2 K/11 (P) SiO_2 and 100 Fe/5 Cu/4.2 K/1.1 (B) SiO_2 have excellent selectivity characteristics (low methane and high C_{5+} yields), but their productivity and stability (deactivation rate) need to be improved. Mechanical integrity (attrition strength) of these two catalysts was markedly dependent upon their morphological features. The attrition strength of the catalyst made out of largely spherical particles (1.1 (B) SiO_2) was considerably higher than that of the catalyst consisting of irregularly shaped particles (11 (P) SiO_2).

3.0 EXPERIMENT

3.1 Catalyst Preparation

A series of spray-dried Fe F-T catalysts having compositions of 100/Fe/5Cu/4.2K/ $x$$SiO_2$ was used in this study. Six catalyst compositions in this series were prepared with precipitated SiO_2 at different levels: 0, 3, 5, 8, 10, and 12 wt% based on total catalyst weight. Fe/P(y) is used to refer to each catalyst composition according to its precipitated SiO_2 content incorporated; for instance, Fe/P(5) refers to the catalyst composition with 5 wt% precipitated SiO_2 added. The concentrations of Cu and K relative to Fe remained identical for all catalyst compositions; therefore, they are not used in the catalyst nomenclature. The details of catalyst preparation can be found elsewhere (7, 28). In brief, a solution containing the desired ratio of $Fe(NO_3)_3 \bullet 9\ H_2O$, $Cu(NO_3)_2 \bullet 2.5\ H_2O$, and $Si(OC_2H_5)_4$ (added to give precipitated SiO_2) was precipitated with ammonium hydroxide. An aqueous potassium promoter $KHCO_3$ was added to a slurry of the precipitate. The slurry was spray-dried at 250^{o}C in a Niro spray drier and was then calcined at 300^{o}C for 5 hours in a muffle furnace. The calcined catalysts were sieved between 38-90 μm before attrition testing and other characterizations.

3.2 Catalyst Characterization

Attrition tests were conducted using a jet cup system. The details of the system configuration as well as test procedure have been extensively described previously (63, 65). In the jet cup test, 5g of each calcined catalyst sample was evaluated for attrition resistance under identical testing conditions using an air jet flow of 15 l/min with a relative humidity of 60 $\pm$5% at room temperature and atmospheric pressure. After one-hour time-on-stream, the air jet flow was stopped and the weight of fines collected by the downstream filter was determined. "Weight percentage of fines lost" was calculated and used as one of the attrition indices. Particle size distribution before and after attrition testing was determined with a Leeds & Northup Microtrac laser particle size analyzer and used to calculate "net change in volume moment," (61-63, 65). Volume moment is a measure of the average particle size.

A Philips XL30 Scanning Electron Microscope (SEM) was used to observe the morphology of the catalyst particles, before and after attrition, and also the structure of the precipitated SiO_2 network in the catalyst particles, after acid leaching. Elemental analysis was carried out to determine surface composition and distribution of each element on cross-sectional

surfaces of catalyst particles using Energy Dispersive X-ray Spectroscopy (EDXS). Powder X-ray Defraction (XRD) patterns of the catalyst samples was determined using a Philips X'pert Diffractometer. Catalyst BET surface areas and pore volumes were measured using a Micromeritics ASAP 2010 automated system. Each catalyst sample was degassed under vacuum at 100^{o}C for one hour and then 300^{o}C for three hours before BET surface area and pore volume measurements. Average particle density (particle mass divided by its volume) of each catalyst was determined using low-pressure mercury intrusion.

4.0 RESULTS

4.1 Catalyst Attrition

Attrition results for all the catalysts studied are summarized in Table 1 and the plot of the two attrition indices, "weight percentage of fines lost" and "net change in volume moment" versus total silica concentration is shown in Figure 1. Weight percentage of fines lost was calculated based on the ratio of the weight of fines collected from the exit filter of the jet cup and the total weight of all particles recovered after the jet cup test. Net change in volume moment was the average particle size change during the attrition test. Since the average particle size decreases during attrition, net change in volume moment is always a positive number. Volume moments of the attritted catalysts were calculated based on both fines generated and particles remaining in the jet cup. Therefore, net change in volume moment is calculated by {[volume moment of fresh – volume moment of attritted (average bottom and fines)]/[volume moment of fresh]} x 100. Detailed calculations and significance of attrition indices have been given elsewhere (61, 63). High values of attrition indices indicate low attrition resistances of catalysts.

As shown in Figure 1, the catalyst without precipitated SiO_2 (Fe/P(0)) showed the highest attrition resistance (least attrition) among all the catalysts tested, while the lowest attrition resistance (highest attrition) was exhibited by the catalysts with the highest concentration of precipitated SiO_2. Figure 1 shows clearly that both attrition indices had similar trends with varying concentration of precipitated SiO_2. Effect of fluidization differences (as a result of particle density differences) on catalyst attrition in the jet cup has been considered and proved to be negligible by using an ultrasonic attrition test, an attrition test with no fluidization involved.

Attrition results from the ultrasonic test were found to be comparable and reproducible within experimental error to those obtained with the jet cup test.

Table 1. Jet Cup Attrition Results

Catalyst	Total SiO_2 Concentration (wt%)	Fines Lost (wt%) [a,b]	Net Change in Volume Moment (5) [c,d,e]
Fe/P(0)	0.0	3.2	6.0
Fe/P(3)	2.7	6.4	18.4
Fe/P(5)	5.2	7.5	23.4
Fe/P(8)	7.6	8.6	27.1
Fe/P(10)	9.9	9.3	30.1
Fe/P(12)	12.1	7.7	27.8
Fe/P(16)	16.1	24.5	--
Fe/P(20)	19.8	29.9	--

(a) Wt% fines = weight of fines collected/weight of total catalyst recovered x 100%

(b) Error = $\pm$10% of the value measured.

(c) Net change in volume moment was determined with reference to the particle size distribution before attrition testing.

(d) Net change in volume moment (VM) = [(VM of sample aF-Ter attrition test – VM of sample before test) / VM of sample before test] x 100%.

(e) Error = $\pm$5% of the value measured.

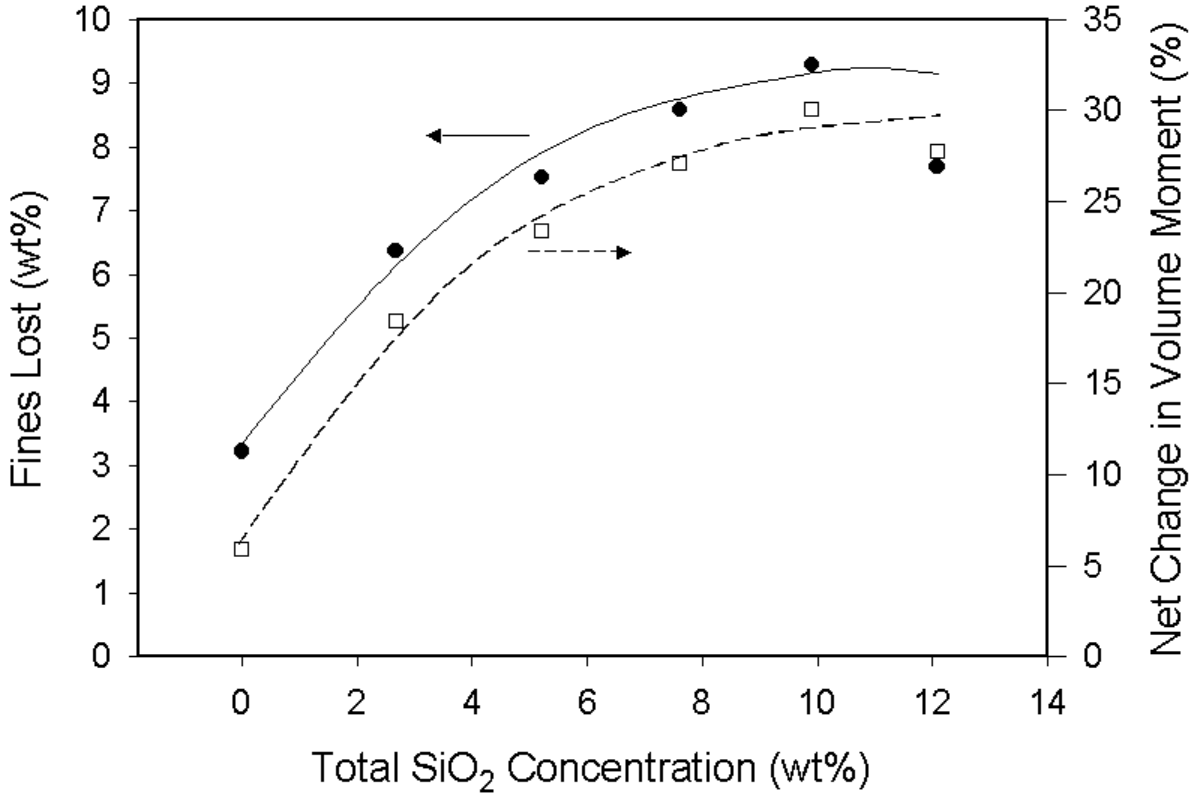

Figure 1. Jet Cup Attrition Results

4.2 Catalyst Particle Properties

The BET surface areas and pore volumes (micro- and meso-pores) of the catalysts, measured by N_2 physisorption, are summarized in Table 2. It can be seen (Table 2) that BET surface areas fluctuated with the total concentration of SiO_2, and no relationship between these two parameters can be drawn. It should be noted that the experimental error of BET surface area measurement is $\pm$5% based on multiple runs of the same sample. However, this error is increased to ca. $\pm$10% by an added sampling error due to potential partial segregation of different particle sizes and densities within a powder sample. In addition, surface area of catalysts may fluctuate somewhat due to slight variations in a number of preparation parameters (especially precipitation pH). As expected, the catalyst with no SiO_2 (Fe/P(0)) had the lowest BET surface area. However, BET surface areas of all the catalysts tested did not change significantly during attrition, except for Fe/P(5) and Fe/P(8). The pore volumes of this catalyst series did not vary significantly with total SiO_2 content and remained essentially unchanged aF-Ter attrition.

The XRD patterns of all the catalysts tested before and after attrition were found to be identical and confirmed that iron existed mainly as hematite (Fe_2O_3). Other components including precipitated SiO_2 were not detectable. The attrition process did not change the XRD patterns of hematite significantly. Thus, as to be expected, attrition affected only physical properties of the catalyst particles and not chemical ones.

Particle density (particle mass divided by its volume including all pore volumes) has been suggested to strongly govern attrition resistance of spray-dried Fe F-T catalysts in calcined, reduced, and carburized forms. Particle density was determined based on low-pressure mercury intrusion in order to prevent mercury from penetrating into the pores of the particles. Mercury porosimetry was used to measure macro pore volumes of the catalyst samples. Particle density and macro pore volume results are summarized in Table 3. It can be seen that macro pore volumes of the selected samples were essentially similar within experimental error. The catalyst with no precipitated SiO_2 (Fe/P(0)) had the highest particle density. Particle density decreased as the concentration of precipitated SiO_2 increased.

Table 2. BET Surface Area and Pore Volume of the Iron Catalysts Studied.

Catalyst	BET Surface Area (m^2/g) [(a)]		Pore Volume (cm^3/g) [(b)]	
	Fresh	Attritted	Fresh	Attritted
Fe/P(0)	24	23	0.08	0.08
Fe/P(3)	69	63	0.12	0.11
Fe/P(5)	83	115	0.12	0.16
Fe/P(8)	48	69	0.11	0.14
Fe/P(10)	41	44	0.11	0.11
Fe/P(12)	76	84	0.11	0.12

(a) Error = $\pm$5% of the value measured.

(b) Error = $\pm$10% of the value measured.

4.3 Catalyst Morphology

SEM micrographs of all the catalyst samples before and after attrition are shown in Figures 2a-c. The catalyst with no precipitated SiO_2 (Figure 2a/Top) shows clearly non-spherical particles while the other catalysts with addition of precipitated SiO_2 have particles that are somewhat more rounded in shape and agglomerated. The figures show that breakage during attrition was mostly a break up of particle agglomerates since there was an obvious decrease in numbers of agglomerates after attrition. There was no evidence to support the actual breakage of distinct catalyst particles. The presence of small chips and pieces caused by abrasion was observed in the fines collected at the top exit of the jet cup. Degree of breakage increased as the amount of precipitated SiO_2 incorporated increased, which is in good agreement with changes in the attrition indices. It can also be observed that some particles had interior holes, seen only as dark spots on particles at higher magnification in Figures 2a-c. Such holes, which have also been found for the spray-dried Fe catalysts studied previously, were probably produced because of the lower efficiency of a laboratory-scale spray drier. Only a small minority of these catalyst particles had holes but the holes provided a means to determine if the silica structure was maintained during acid leaching of the catalyst particles. This will be discussed in detail later.

To obtain a better understanding of the factors affecting attrition resistance, catalyst inner structure as well as distribution of each element in the catalyst particles is important to determine. The distribution of each element in the catalyst particles was determined using EDXS to analyze the cross-sectional area of catalyst particles prepared by microtoming. The elemental mapping results, an example being shown in Figure 3, were found to be similar for all catalyst compositions containing precipitated SiO_2. Iron, Cu, and precipitated SiO_2 were found to be evenly distributed throughout the catalyst particles. Potassium, on the other hand, was found in higher concentrations, at catalyst surfaces as seen on the outer edge of the cross-sectioned particles.

Table 3. Macro Pore Volume and Particle Density of Selected Iron Catalysts.

Catalyst	Macro Pore Volume (cm^3/g) [(a)]	Particle Density (g/cm^3) [(b)]
Fe/P(0)	0.25	1.64
Fe/P(10)	0.26	1.40
Fe/P(12)	0.24	1.44
Fe/P(16)	--	0.81
Fe/P(20)	--	0.79

(a) Measured using mercury porosimetry, error = $\pm$10% of the value measured.

(b) Determined using low-pressure mercury displacement, error = $\pm$5% of the value measured.

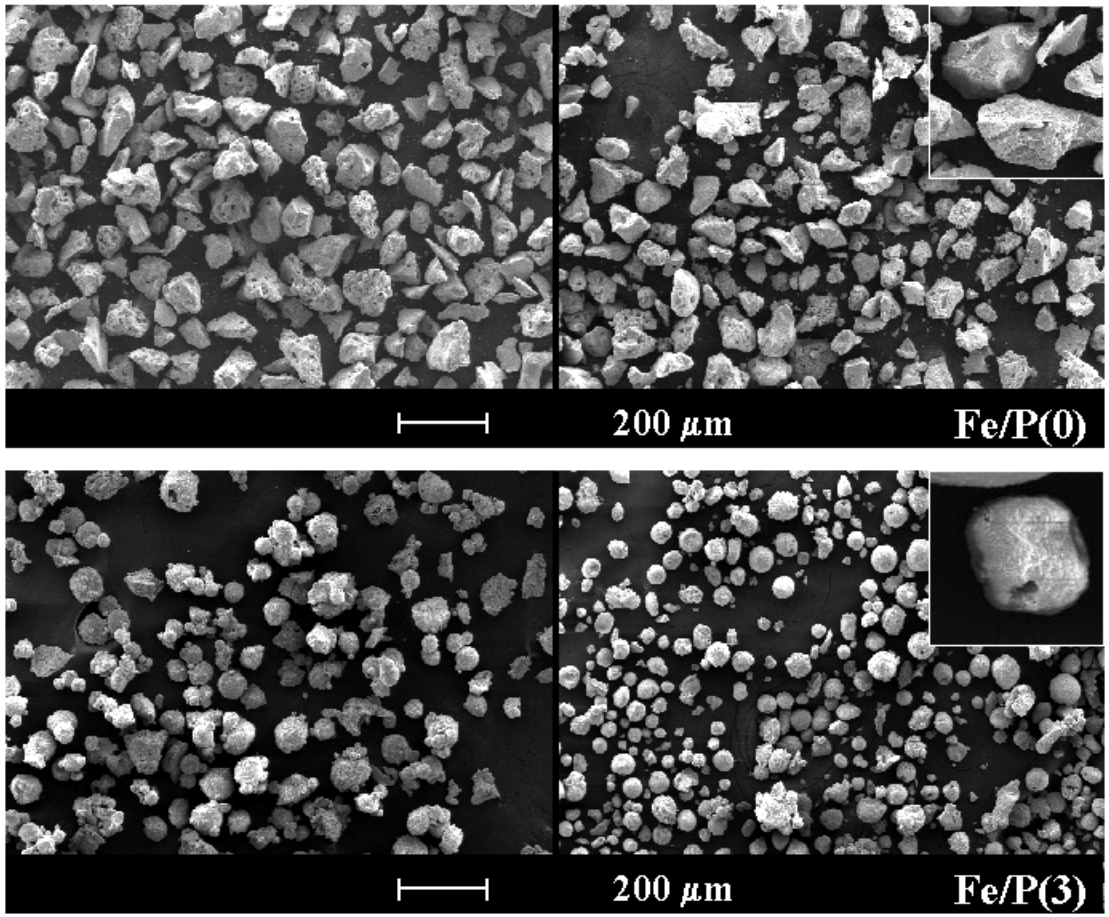

Figure 2a. SEM micrographs of Fe/P(0) and Fe/P(3) before and after attrition.

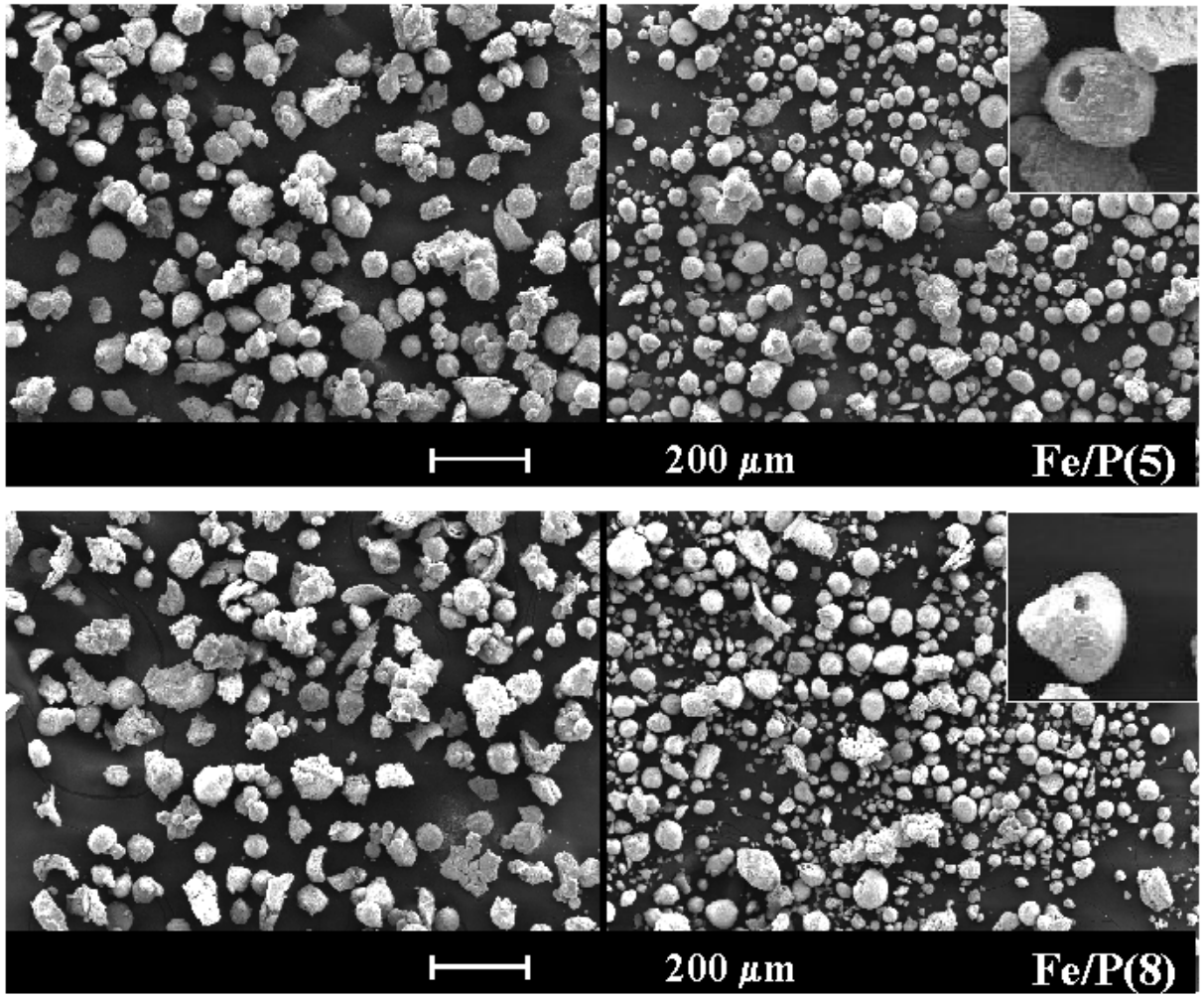

2b. SEM micrographs of Fe/P(5) and Fe/P(8) before and after attrition.

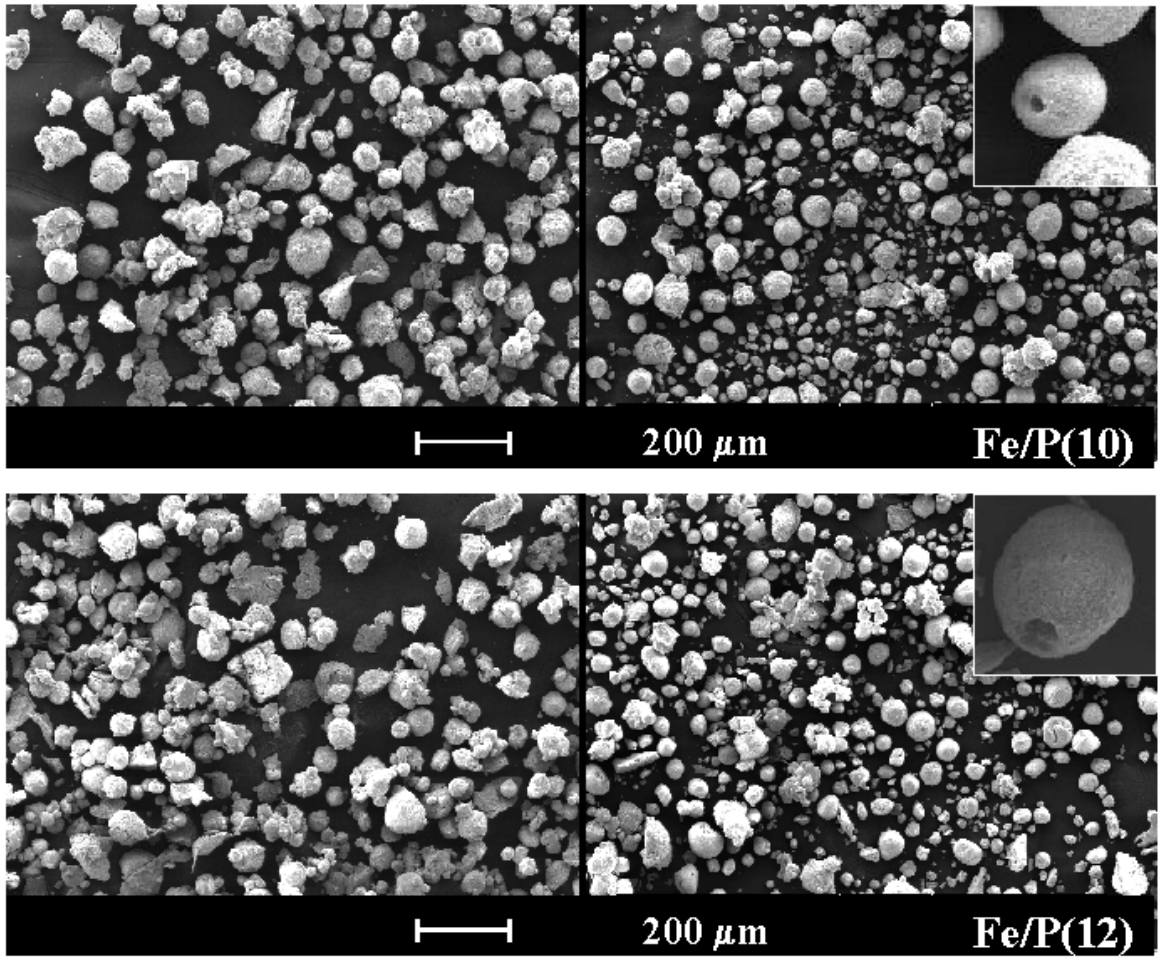

Figure 2c. SEM micrographs of Fe/P(10) and Fe/P(12) before and after attrition.

The precipitated SiO_2 network incorporated in the catalysts can be seen by SEM after acid leaching, which dissolves Fe, iron oxide, Cu, and K and leaves mainly the SiO_2 structure. Catalyst particles were treated with 30% hydrochloric acid (HCl) solution (pH=1) for 48 hours to ensure that those elements were fully removed. The residue was washed thoroughly with deionized water under vacuum filtration and dried under vacuum at room temperature to avoid agglomeration by heating. Figure 4 shows typical SiO_2 structures seen with and without interior holes. Both structures showed a smoother texture of SiO_2 surface at this magnification, which differs from the more porous SiO_2 structures seen in the spray-dried Fe catalysts prepared earlier with either binder or binder + precipitated SiO_2 (28). The SiO_2 structures obtained by leaching catalysts after attrition were identical which is consistent with the fact that there was minimal attrition most was due to a break up of agglomerates (Figures 2a-c).

5.0 DISCUSSION

5.1 Catalyst Attrition Resistance

Although 'weight percentage of fines lost' and 'net change in volume moment' are both used as attrition indices, they have different physical meanings. While weight percentage of fines lost is a representative of the amount of fines generated and elutriated (CA. <22 μm), net change in volume moment represents a change of volume mean average particle size, weighted mostly towards the larger particles (61). Therefore, a combination of these two attrition indices have been used in these attrition studies to help delineate physical attrition both by fracture (generating large broken particles) and abrasion/erosion (generating fines). Due to the difference in their physical meanings, it would not be surprising if the values of these two parameters were not identical with each other. However, for this spray-dried Fe catalyst series prepared with precipitated SiO_2 only, both attrition indices show similar trends in their relationship to the amount of precipitated SiO_2 added (Figure 1). These results suggest that the change in average particle size (mostly large particles) occurred in a similar degree as fines generated and possibly that the breakage of large particles facilitated the generating of fines. Weight percentage of fines lost is, however, considered the most important attrition index in these studies since fines

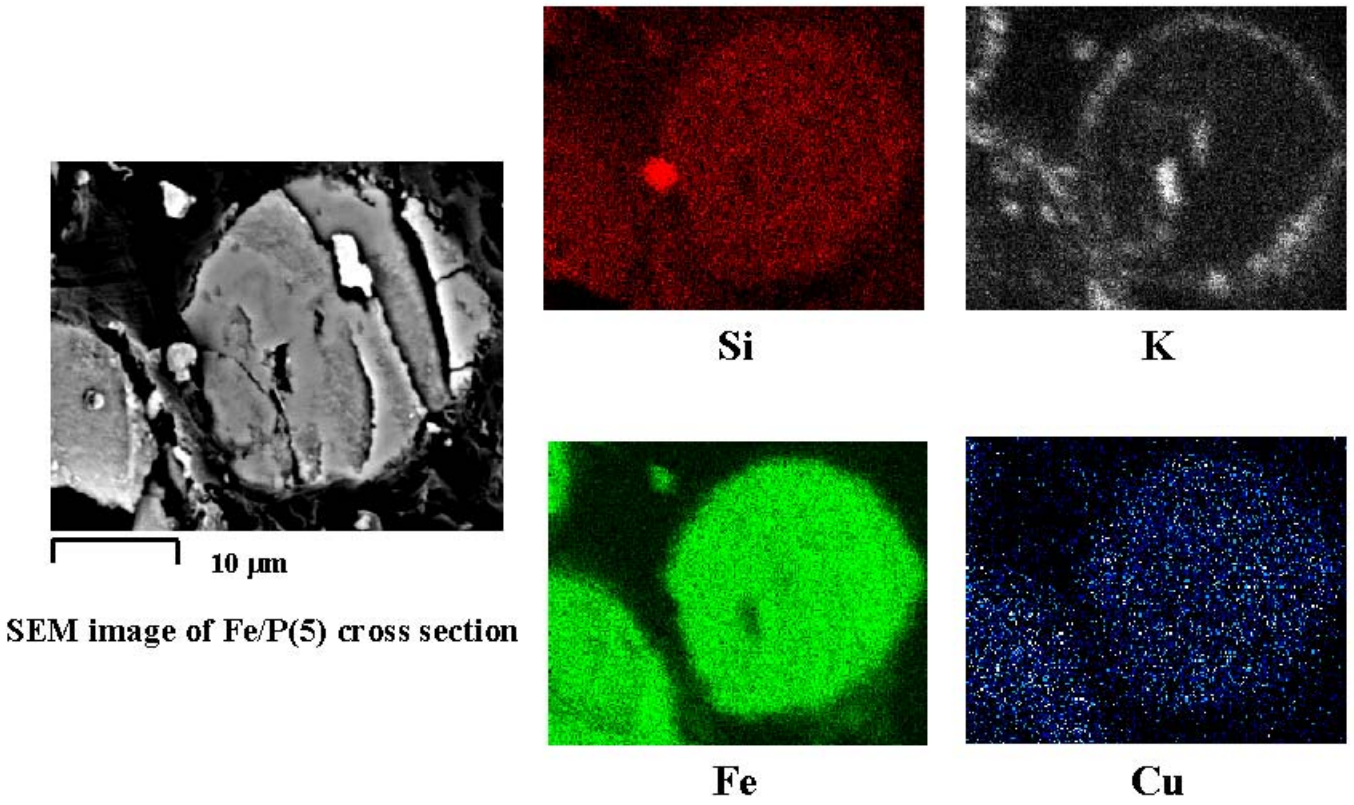

Figure 3. EDXS results for the cross section of a typical Fe/P(5) particle.

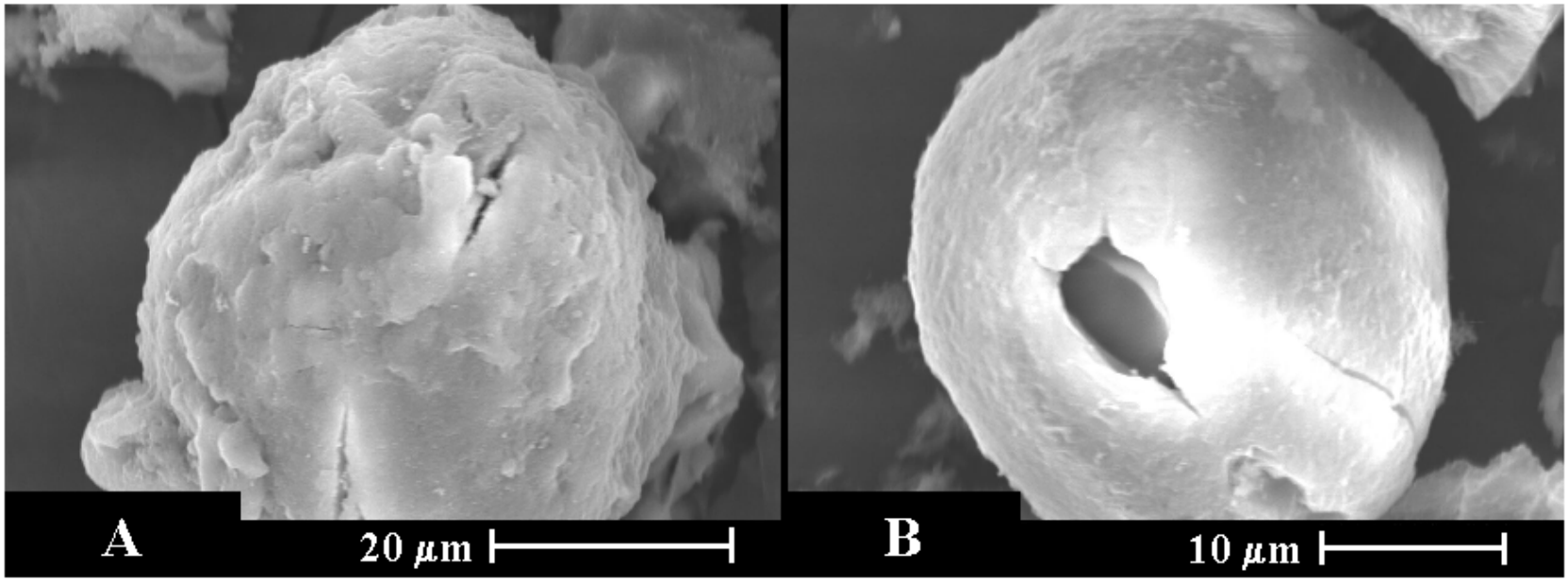

Figure 4. SEM micrographs of typical SiO_2 structures after acid leaching [Fe/P(12)]: (A) typical structure, (B) particle with interior.

generated caused the aforementioned problems in SBCR operation and since these catalysts were developed for SBCR usage.

In a previous study (61) to determine the effect of SiO_2 type (binder vs. precipitated + binder) and concentration on attrition resistance of spray-dried Fe catalysts, the catalyst having only binder SiO_2 (Fe/P(0)/B(11)) at the moderate concentration of CA. 11 wt% SiO_2 showed the highest attrition resistance (least attrition). Addition of precipitated SiO_2 to this composition (Fe/P(*y*)/B(10)) was found to reduce attrition resistance sharply. The use of precipitated silica alone at high loadings (20-25 wt%) is well known to result in poor attrition resistant Fe catalysts. However, the effect of having only precipitated SiO_2 at lower concentrations, especially in spray-dried Fe catalysts, was not determined. Thus, it is useful to compare the attrition results of the catalysts in this study (which had the same Fe/Cu/K ratios as those previously studied but were prepared with only precipitated SiO_2) with those from the previous study (61) (see Figure 5). Catalysts with only precipitated SiO_2 at concentrations <12 wt% showed significantly improved attrition resistance than other catalyst compositions. At a moderate total SiO_2 concentration about 11 wt%, the curves for the three catalyst series essentially intersect, indicating that some particle property of these spray-dried iron (Fe) catalysts prepared with similar amounts but different types of SiO_2 could possibly have an influence on their attrition resistances.

The two catalysts having the lowest concentrations of binder SiO_2 seem to have had somewhat different attrition properties than the rest of the catalysts (Figure 5). This was possibly due to their being prepared at different solution pH and/or drying temperature, which may have caused lower particle densities than otherwise expected. This effect has been shown to be reproducible.

In the earlier studies (61, 64), catalyst attrition was found to depend greatly on catalyst particle density and that this was not due to a bias in the attrition test. Figure 6 shows % fines lost versus particle density for catalysts prepared with only precipitated SiO_2 and for catalysts prepared with only binder SiO_2 or with binder + precipitated SiO_2 (2). The results for the catalysts having only precipitated SiO_2 are completely consistent with the previous data and therefore confirm the strong relationship between these two parameters. Thus a catalyst with a high particle density exhibits low attrition or, in other words, has high attrition resistance. On the other hand, very dense catalysts, however, may not be fluidized well enough to obtain a good dispersion in a reactor slurry, leading to poor contact between reactants and catalyst particles.

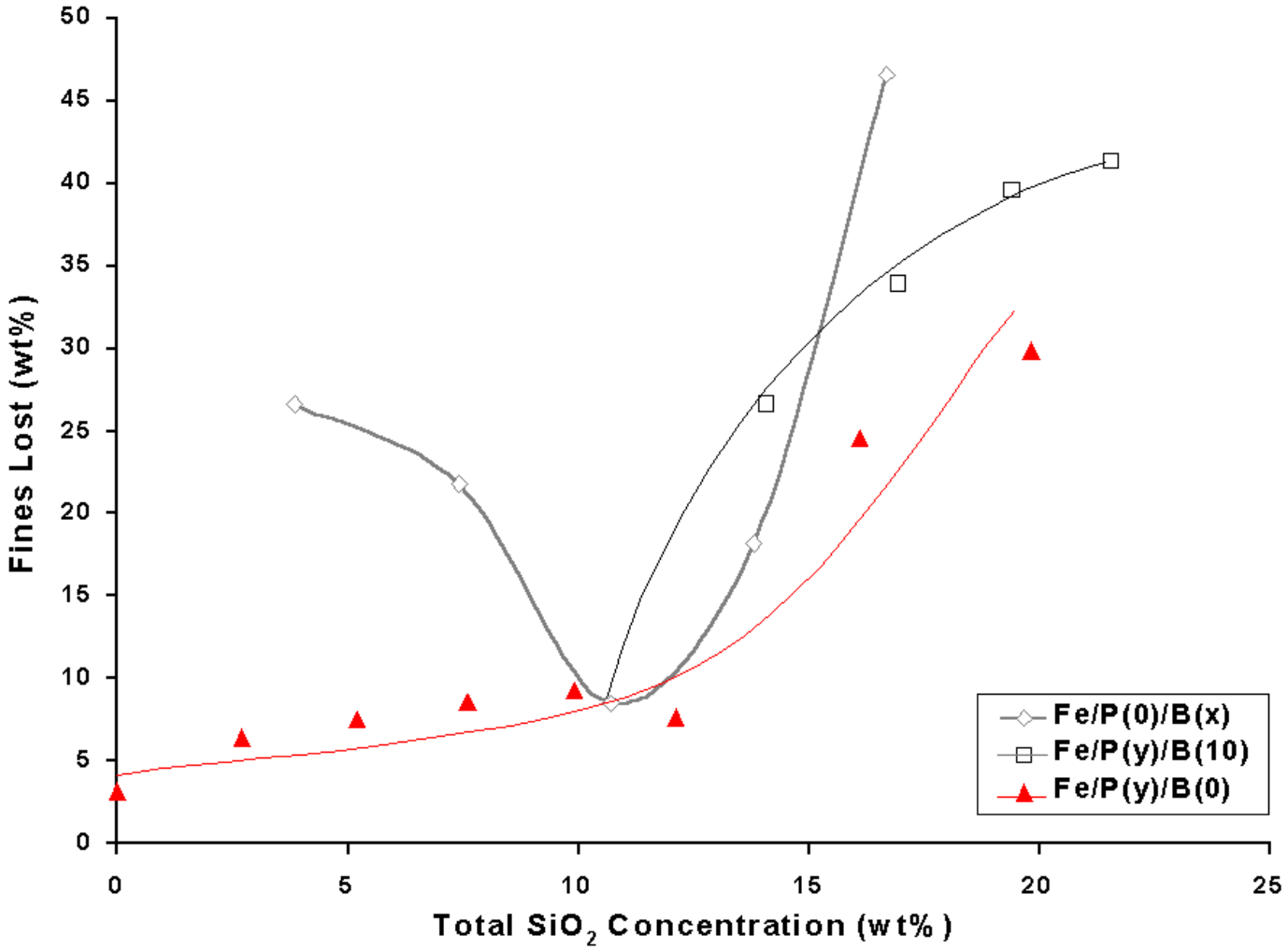

Figure 5. Weight percentage of fines lost vs. total concentration of SiO_2 for different series of spray-dried Fe F-T catalysts: B refers to binder SiO_2; P refers to precipitated SiO_2; *x* and *y* refer to the amount of binder and precipitated SiO_2 added, respectively. [Data for Fe/P(0)/B(*x*) and Fe/P(*y*)/B(10) from ref. 1].

Thus, attrition resistance is not only the important factor in catalyst design for SBCR usage. High surface area and proper particle density are also needed to obtain high catalytic activity and good fluidization, respectively. The presence of SiO_2 in Fe F-T catalysts enhances the active surface areas but lowers the density of the catalyst as well as the attrition resistances. Therefore, the amount of SiO_2 added must be optimized to obtain high catalytic activity, high attrition resistance, and good fluidization of catalyst particles when used in SBCRs.

5.2 SiO_2 Structure

AF-Ter acid leaching, precipitated SiO_2 particles (Figure 4) were not found to be significantly changed in either size or shape from the original catalyst particles. Moreover, those particles with interior-hole structures maintained the same structure (with holes) aF-Ter being acid leached. All these observed structures after acid leaching as well as the EDXS results suggest that the structure of precipitated SiO_2 in the catalyst particles was a continuous network (skeleton). There is no evidence that suggests the SiO_2 existed as discrete, non-continuous parts in the original catalyst particles that somehow agglomerated during acid leaching. Although some SiO_2 particles were found to have interior holes, in no way did they have an'egg shell' structure. Precipitated SiO_2 was evenly distributed, as shown by EDXS (Figure 3), throughout the particles, similarly to Fe.

The surface morphology of the acid leached precipitated SiO_2 particles (Figure 4) both with and without interior holes was relatively more smooth compared to the porous SiO_2 structures resulting from acid leaching of the catalysts prepared with binder SiO_2 or binder + precipitated SiO_2 [2] . However, the difference in this morphology did not seem to be a major factor for the physical strength of the catalysts (Figure 5).

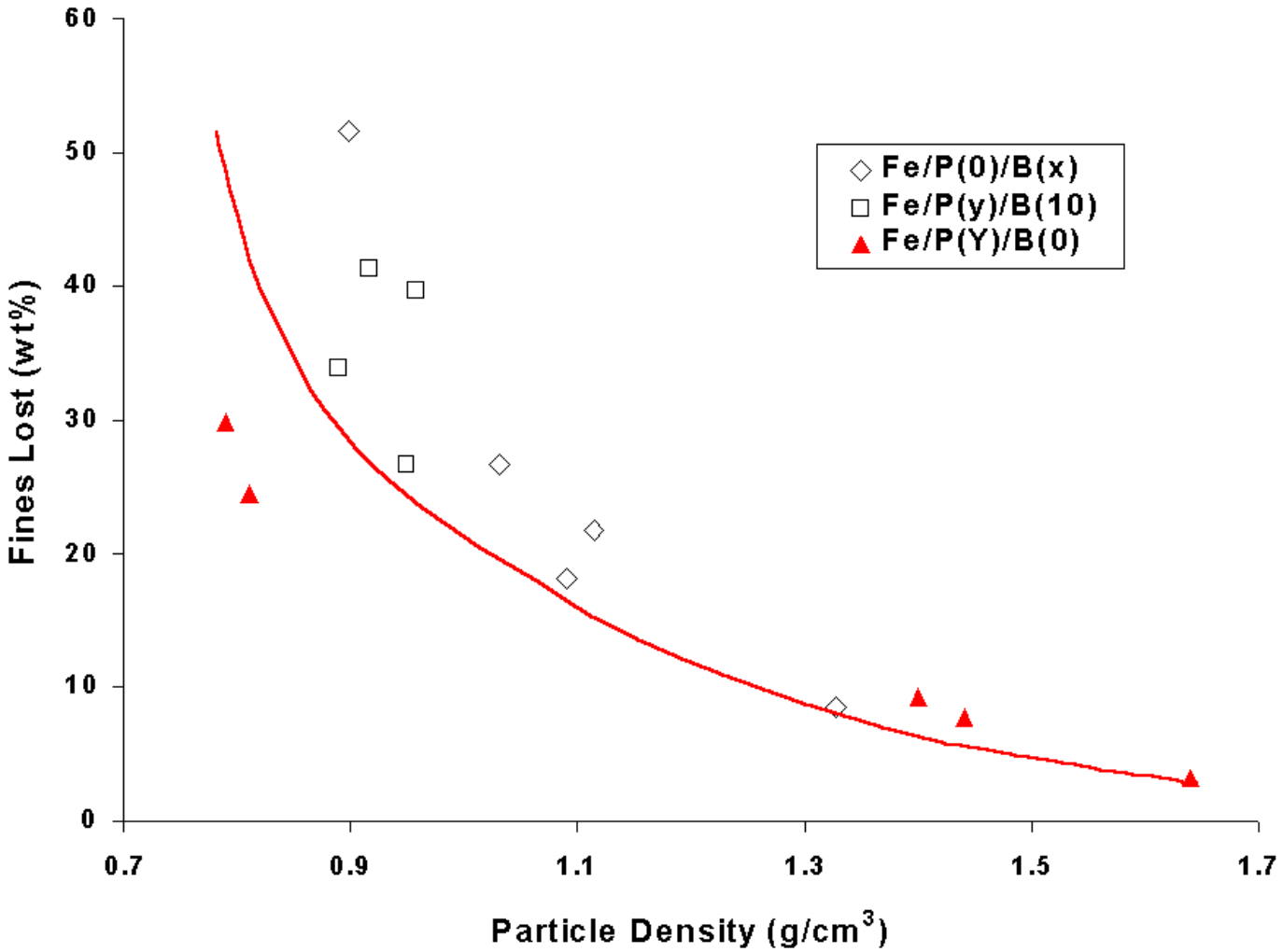

Figure 6. Weight percentage of fines lost vs. average particle density of calcined Fe/P(*y*), Fe/B(*x*), and FE/P(*y*)/B(10) catalysts.

5.3 Slurry Reactor Tests

Two catalysts were used in the present study with the following compositions: 100 Fe/5 Cu/4.2 K/1.1 (B) SiO_2 (designated as Catalyst B, since it contains binder silica) and 100 Fe/5 Cu/4.2 K/11 (P) SiO_2 (Catalyst P, containing precipitated silica). Compositions are given in parts by weight, except for the silica content, which represents weight percent of silica in the fresh catalyst (based on total catalyst weight).

The reactor testing was conducted at Texas A & M University and The Center for Applied Energy Research of the University of Kentucky. Details of the reactor tests such as experimental set up, operating procedures and product quantification can be found elsewhere (14, 17). A brief description of experimental apparatus is summarized here. Experiments were conducted in a 1-dm^3 stirred tank reactor (Autoclave Engineers, Erie, Pennsylvania). A standard six-blade turbine impeller of 3.2 cm in diameter and a stirrer speed of 1200 rpm were used in all experiments. The feed gas flow rate was adjusted with a mass flow controller and passed through a series of oxygen removal, alumina, and activated charcoal traps to remove trace impurities. After leaving the reactor, the exit gas passed through a series of high and low (ambient) pressure traps to condense liquid products. High molecular weight hydrocarbons (wax), withdrawn from the slurry reactor through a porous cylindrical sintered metal filter, and liquid products, collected in the high and low pressure traps, were analyzed by gas chromatography. The reactor was charged with ~15 g of as-received catalyst dispersed in approximately 400 g of Durasyn-164 oil (hydrogenated 1-decene homopolymer). Slurry samples were withdrawn from the reactor at TOS = 0 hours (TOS = time on stream) and at the end of the test. Durasyn-164 oil (or hydrocarbon wax produced during F-T synthesis) was removed by filtration aided by the addition of a commercial solvent, Varsol 18 (a mixture of liquid aliphatic and aromatic hydrocarbons).

Catalysts were reduced *in situ* with CO at 280^{o}C, 0.8 MPa, 3 NL/(g-cat·h) (where NL/h denoted volumetric gas flow rate at 0^{o}C and 1 bar) for 12 hours. AF-Ter the pretreatment, the catalysts were initially tested at 260^{o}C, 2.1 MPa, H_2/CO = 2/3, and gas space velocity of 3.5 NL/(g-Fe·h).

5.4 Catalyst Activities and Selectivity in Stirred Tank Slurry Reactor (STSR)Tests

Results from tests conducted with precipitated catalyst and binder catalyst are shown in Figures 7-14. The catalysts were pretreated under the same conditions, and the process conditions were similar in both tests except for a 110-h time-period (224-334 h) in the case of precipitated iron silica when a significantly higher gas space velocity was employed.

In both tests, during the first 50-80 h on stream, the syngas conversion increased with time reaching 85-87%. After reaching the maximum conversion, the catalysts started to deactivate and at 200 h on stream the syngas conversion was about 76% in both tests. During the first 200 h of testing, the syngas conversion values were about the same in both tests. Since the gas hourly space velocity in the test employing binder silica was lower than that used in precipitated silica (3.1 vs. 3.5 NL/g-Fe · h), it was concluded that the intrinsic activity of precipitated catalyst is higher than that of binder catalyst.

In test employing precipitated silica catalyst, the gas hourly space velocity was increased to 5.2 NL/g-Fe · h at 224-h on stream, which was accompanied by decrease in conversion and further catalyst deactivation between 225 and 280 hours on stream. Between 280 and 334 hours, the conversion was fairly stable (43-44%). AF-Ter returning to the baseline conditions at 335 h, the syngas conversions were about 60%, but the activity continued to decrease with time and at the end of the run (384 h) the conversions were about 48%. The average loss in syngas conversion (catalyst deactivation rate) between 80 and 224 hours was 0.09%/hour, whereas the average conversion loss for the time period between 80 and 384 hours was 0.145%/hour (3.84%/day). This shows that catalyst deactivation was faster during the latter portion of the test.

In test employing binder silica catalyst, the process condition was constant. After 204-h on stream, the syngas conversion decreased abruptly from 78% to 66%, and remained at this lower value during the next 40 hours of testing. This drop in conversion was probably caused by a reduction in stirring rate, due to malfunctioning of an electric motor. At 247-h the test was suspended due to complete stoppage of the stirrer. During the test interruption, the catalyst was kept in a N_2 atmosphere at 120^{o}C for 30 days. After the test was resumed, the initial conversion was similar to that observed at 204 h, i.e.,

before the problem with the electric motor arose. However, the catalyst activity continued to decrease with time reaching 60% at the end of the test (449 h). The average rate of catalyst activity loss between 53 and 449 h was 0.0676%/hour (1.62%/day), which is significantly smaller than that observed in the precipitated catalyst situation.

Both catalysts exhibited very high water gas shift (WGS) activity. Selectivity to CO_2 increased quickly with time reaching a stable value of about 49% (not shown). The WGS activity remained stable throughout the test, even though the F-T activity decreased with time.

Hydrocarbon selectivities (CH_4 and C_5+) were similar in both tests. Methane selectivity (carbon atom basis) decreased during the first 150 h of testing, reaching a fairly stable value of 2.0 $\pm$ 0.2%. Methane selectivity was not markedly affected by changes in conversion and/or process conditions. Selectivity of C_5+ hydrocarbons (liquids and wax) was high in both tests, increasing to 84-86% during the first 130-150 hours of testing and then decreasing somewhat after about 200 h on stream. Liquid plus wax selectivity (fraction of C_5+ hydrocarbons among total hydrocarbons on carbon atom basis) was also not markedly affected by changes in conversion level and/or process conditions.

6.0 Conclusion

Spray-dried catalysts with compositions 100 Fe/5 Cu/4.2 K/11 (P) SiO_2 and 100 Fe/5 Cu/4.2 K/1.1 (B) SiO_2 investigated in STSR have excellent selectivity characteristics (low methane and high C_5+ yields), but their productivity and stability (deactivation rate) need to be improved. Mechanical integrity (attrition strength) of these two catalysts was markedly dependent upon their morphological features. The attrition strength of the catalyst composed of largely spherical particles (1.1 (B) SiO_2) was considerably higher than that of the catalyst consisting of irregularly shaped particles (11 (P) SiO_2). Improvements in spray drying operating parameters resulting in narrower particle sized distribution (PSD) and higher sphericity could lead to further improvements in the attrition strength.

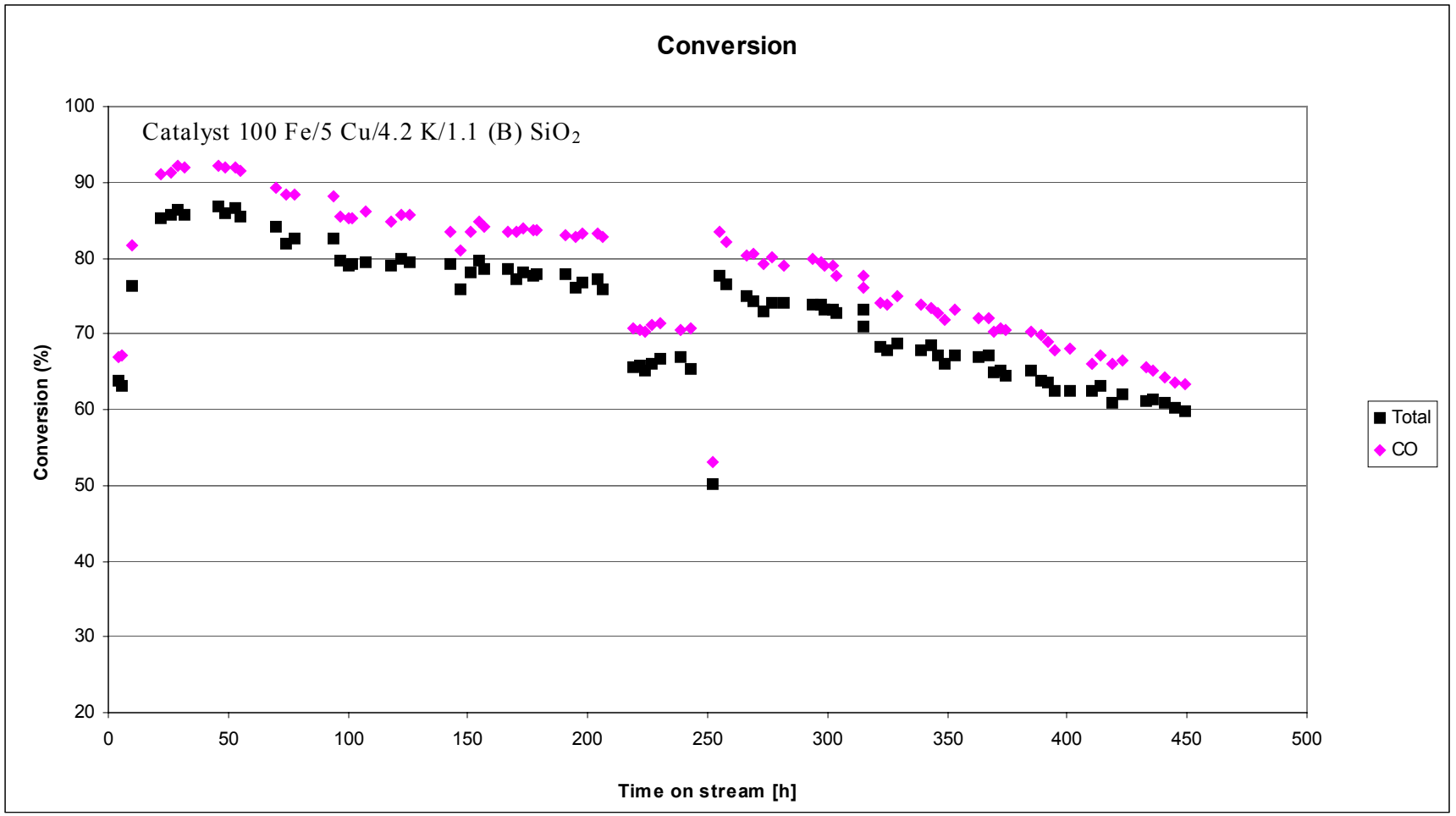

Figure 7. Syngas Conversion with Time On-Stream for Binder Silica

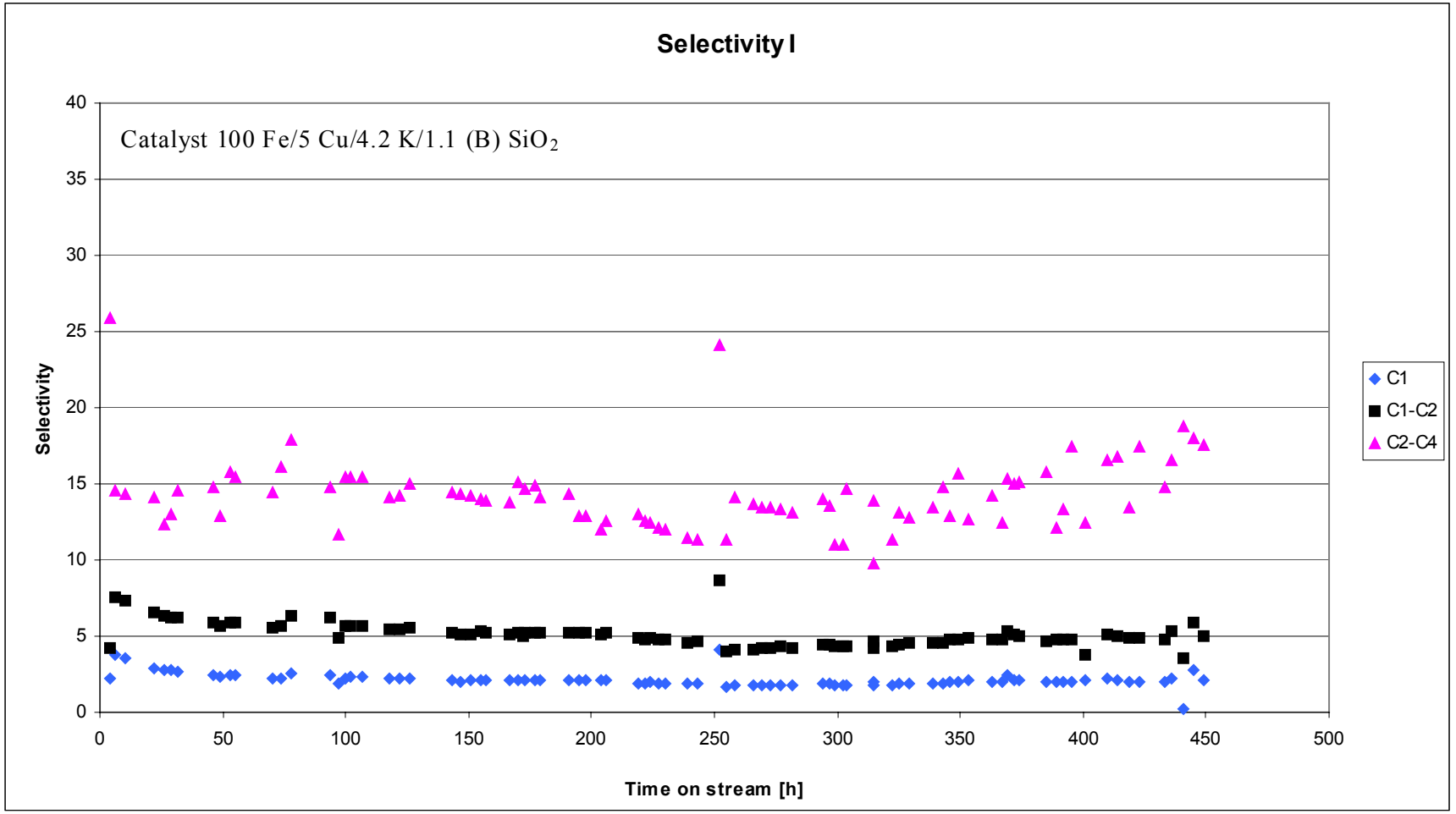

Figure 8. C_1-C_4 Selectivity with Time on stream for Binder Silica.

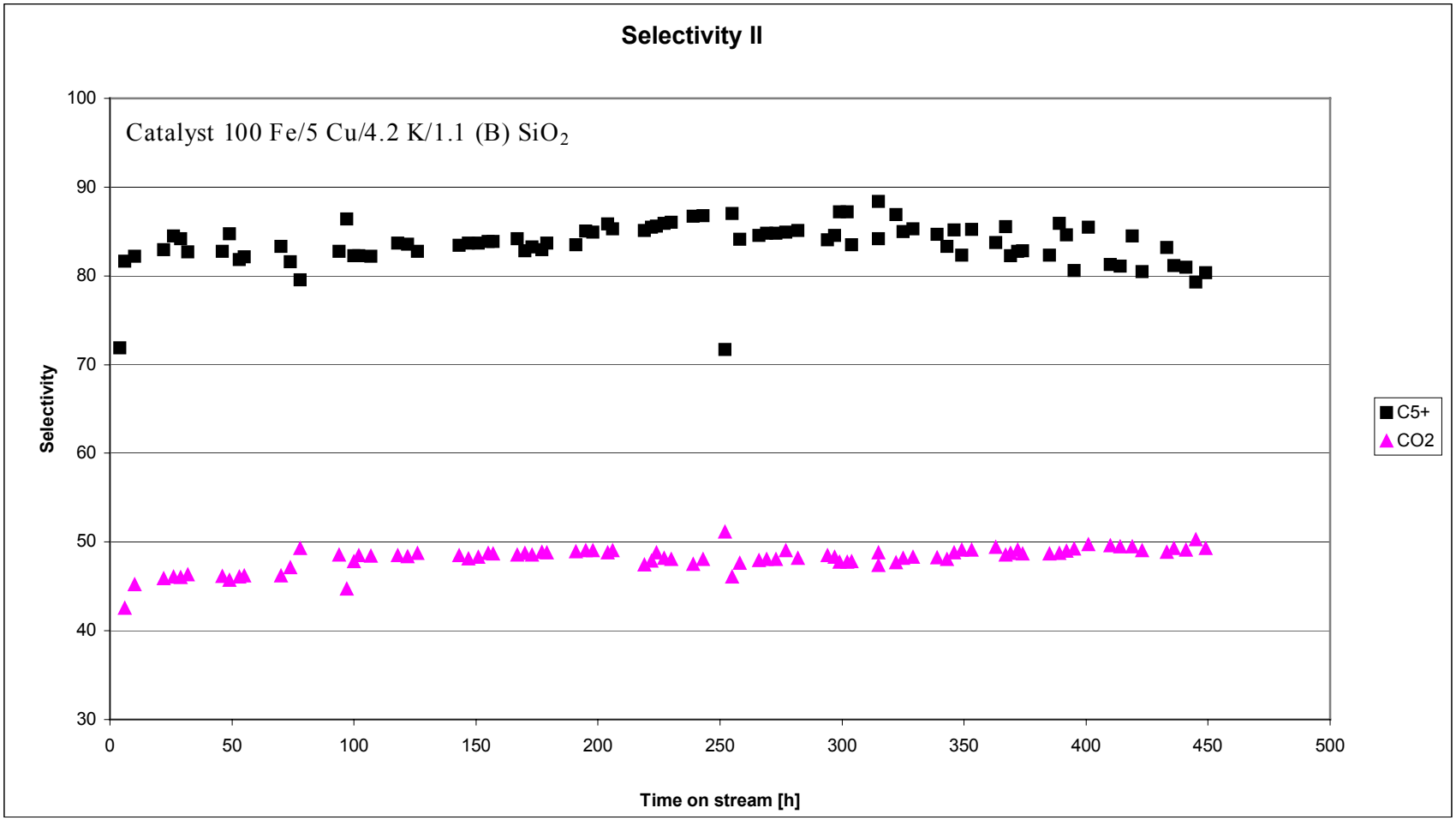

Figure 9. C_5+ Selectivity with Time on Stream for Binder Silica.

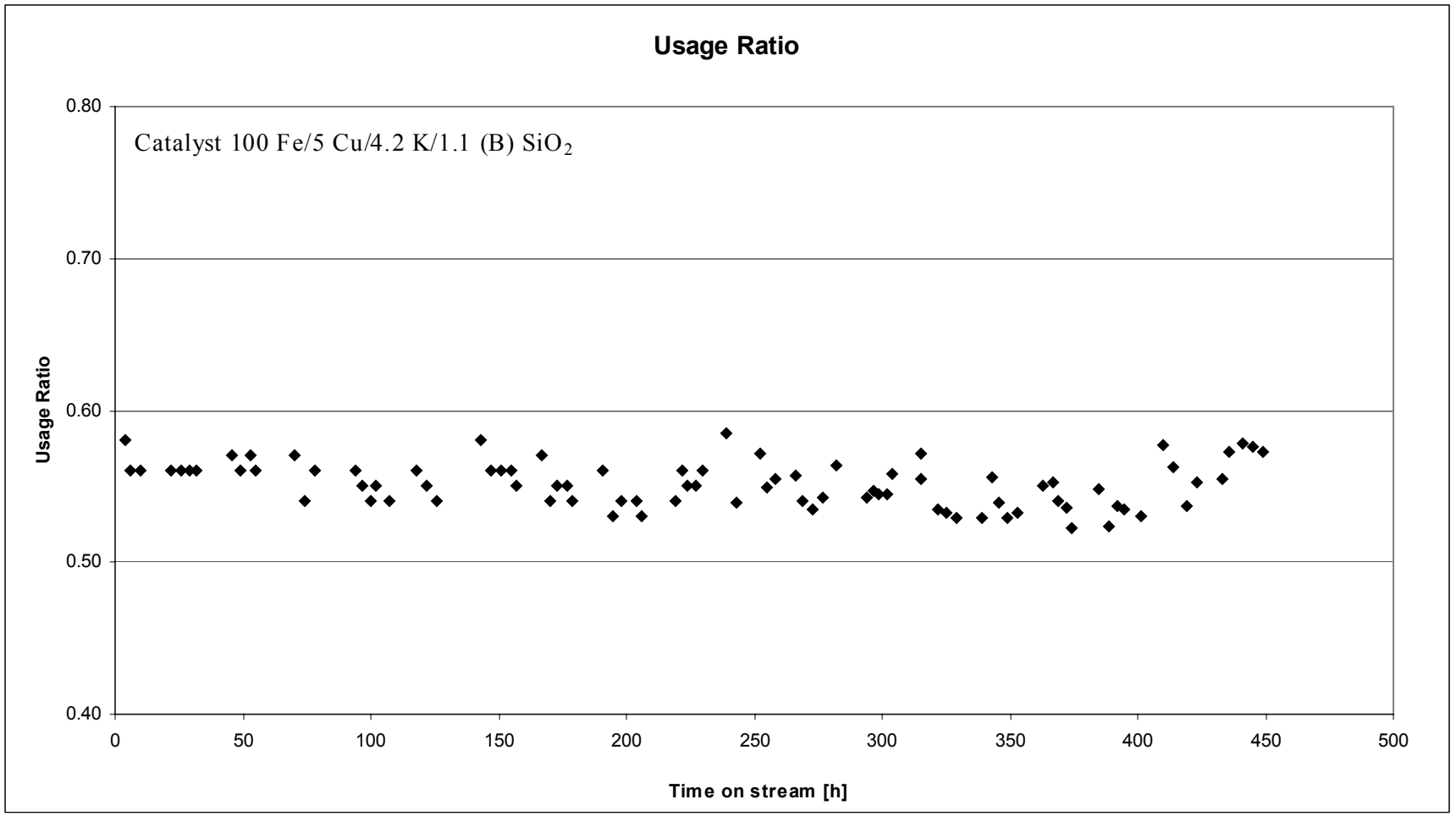

Figure 10. Usage Ratio with Time on Stream for Binder Silica.

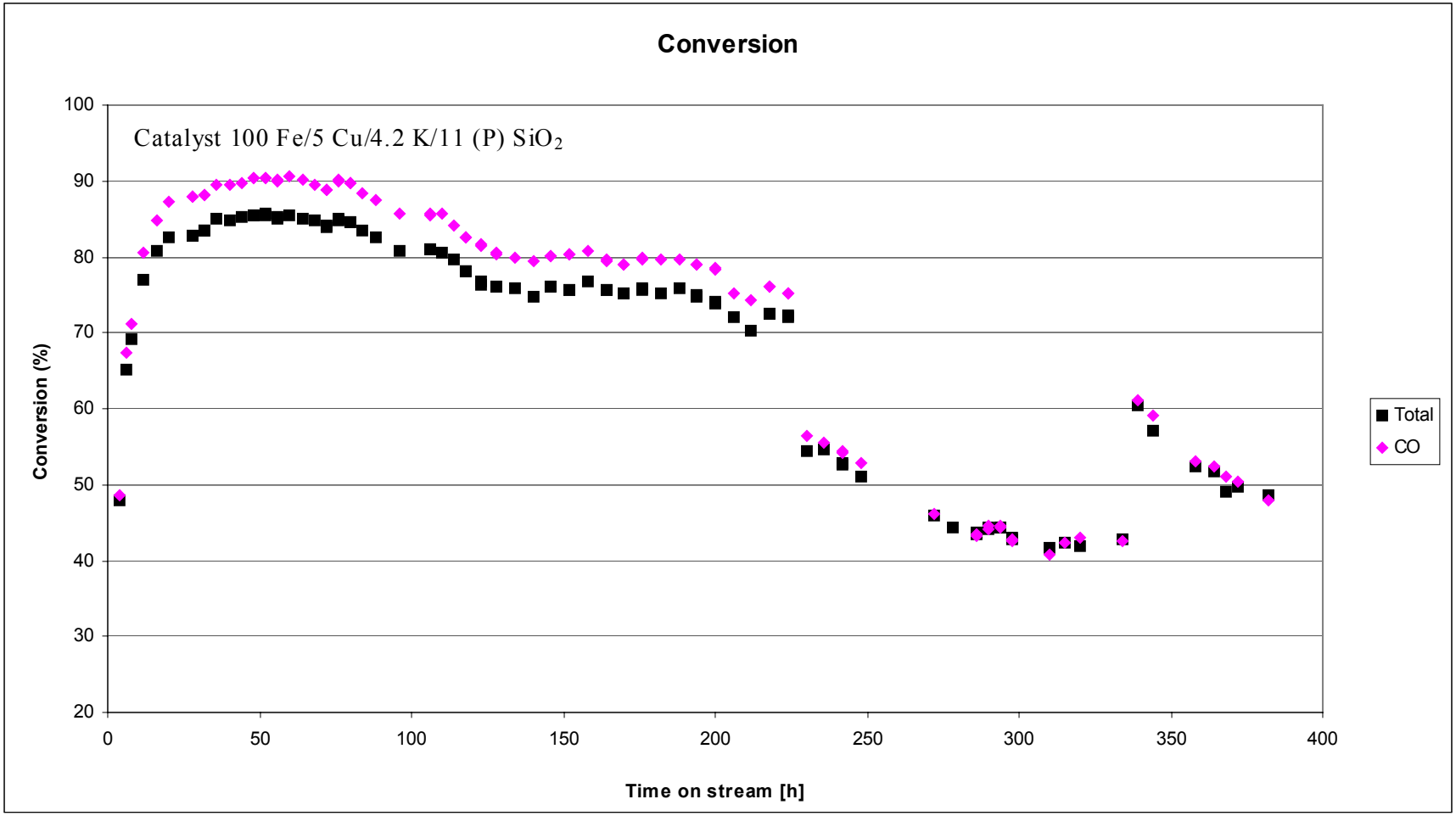

Figure 11. Syngas Conversion with Time On-Stream for Binder Silica.

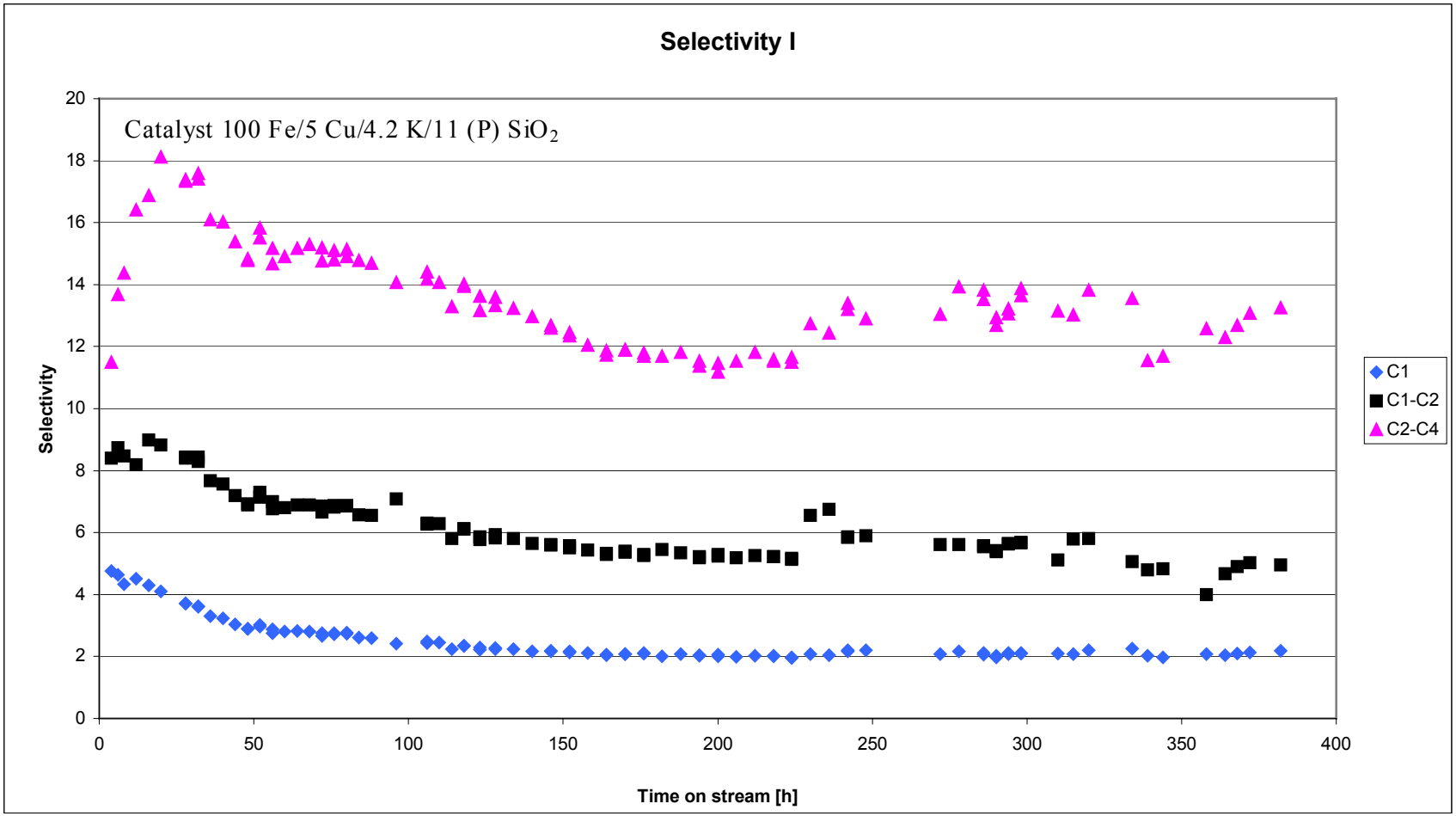

Figure 12. C_1-C_4 Selectivity with Time On-Stream for Precipitated Silica.

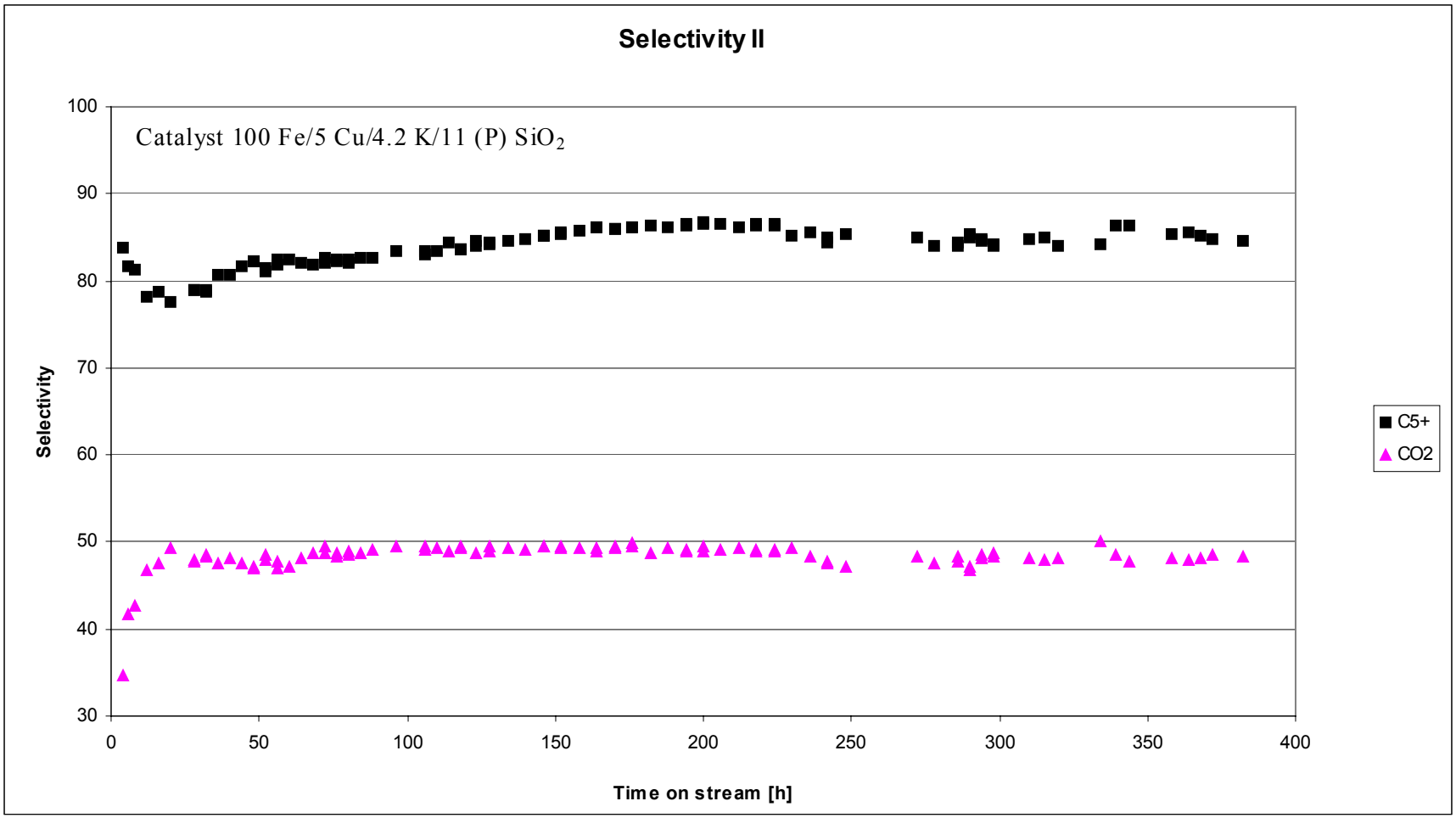

Figure 13. C_5+ Selectivity with Time On-Stream for Precipitated Silica.

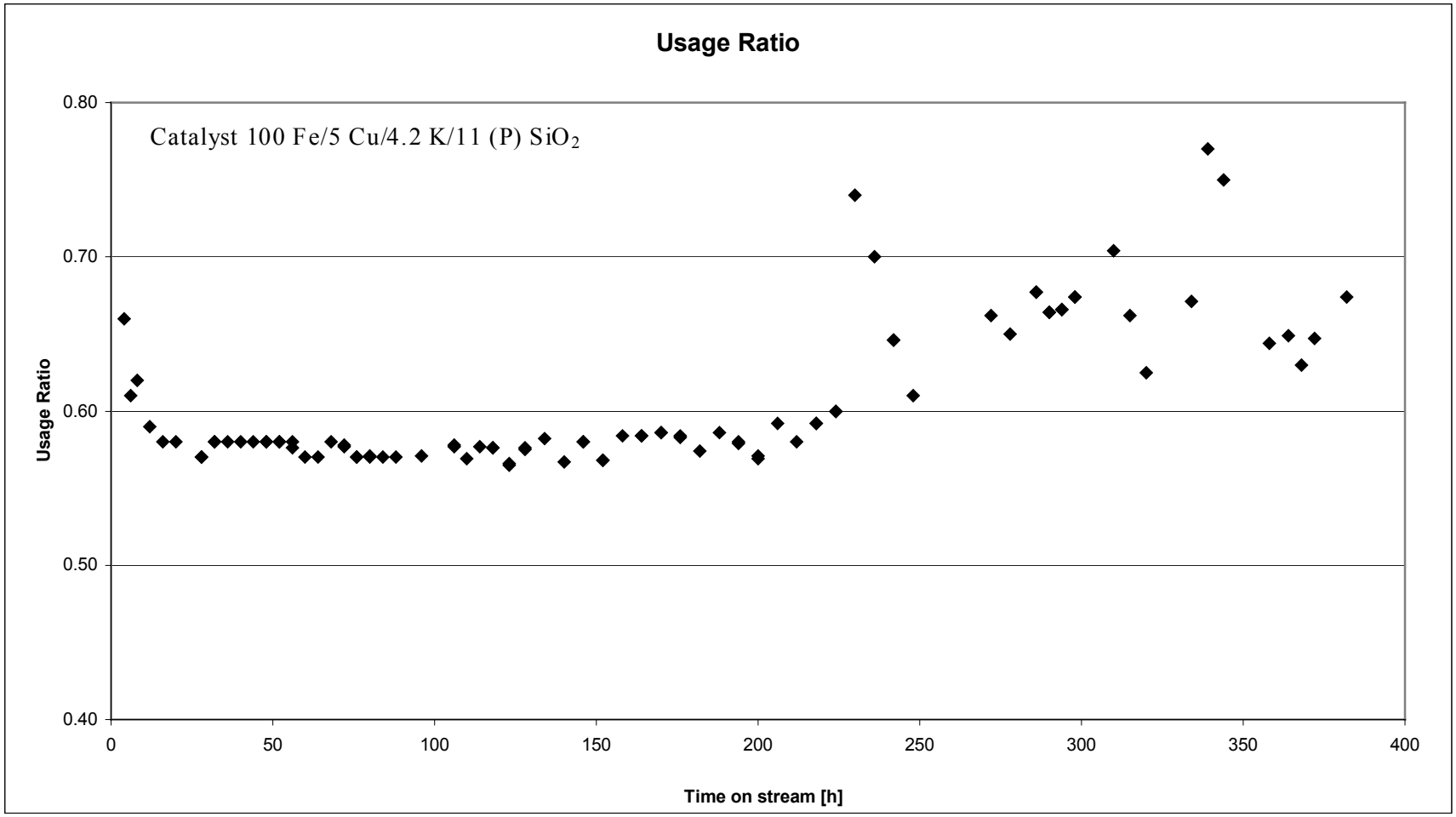

Figure 14. Usage Ratio with Time On-Stream for Precipitated Silica.

100Fe/5Cu/4.2K/11(P)SiO_2

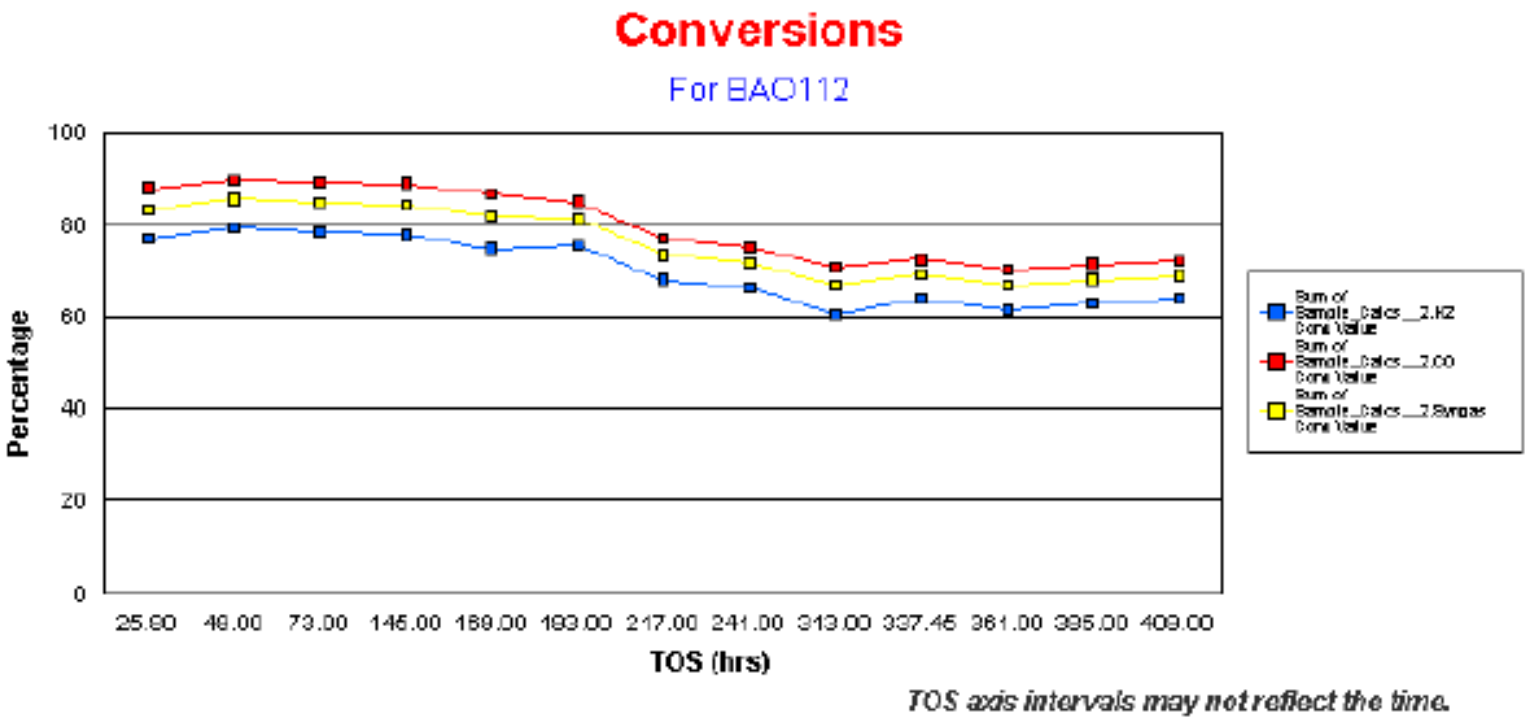

Figure 15. Syngas conversion with the on-stream for precipitated silica, CAER data.

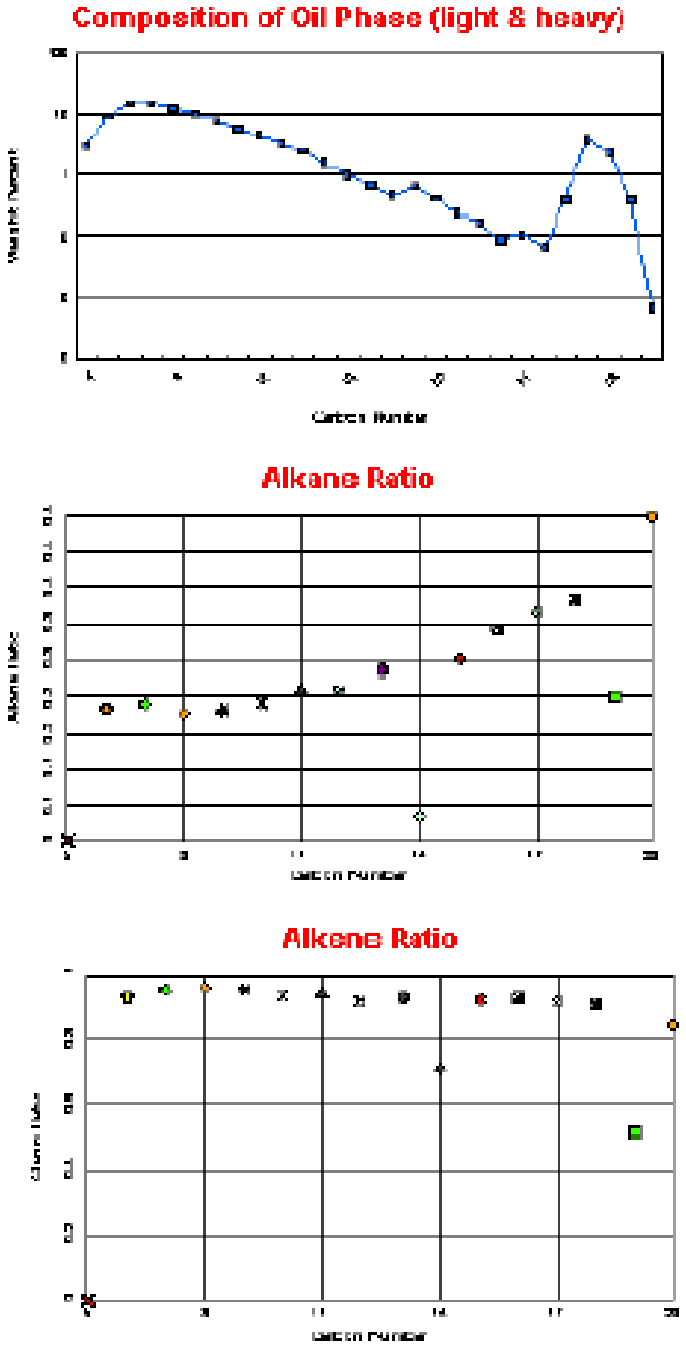

Figure 16. Oil Phase Distribution Precipitated Silica, CAER data.

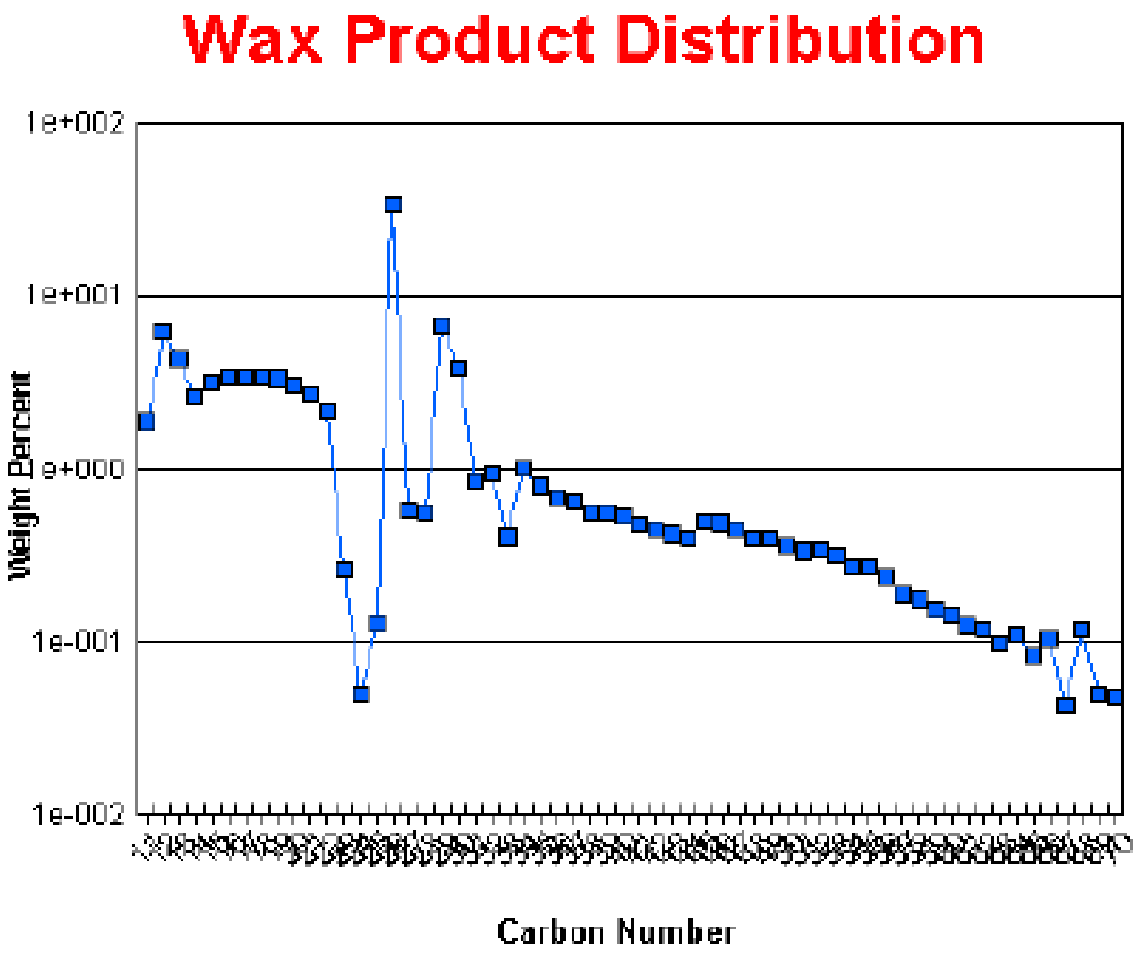

Figure 17. Wax Product Distribution Precipitated Silica, CAER data.

Cat: DOE002 1.1Fe/5Cu/4.2K/1.1BsiO2 Catalyst

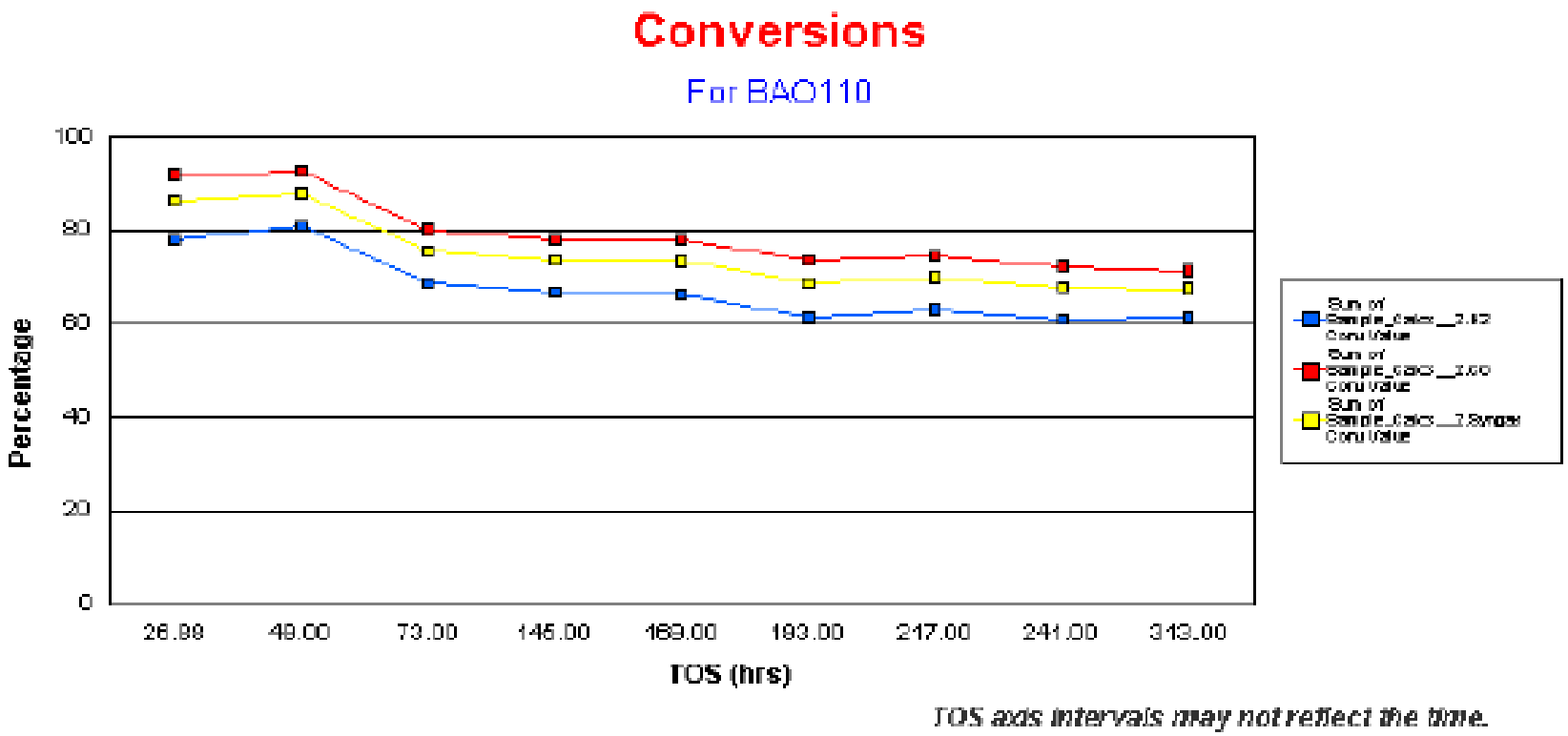

Figure 18. Syngas Conversion with Time On-Stream for Binder Silica, CAER data.

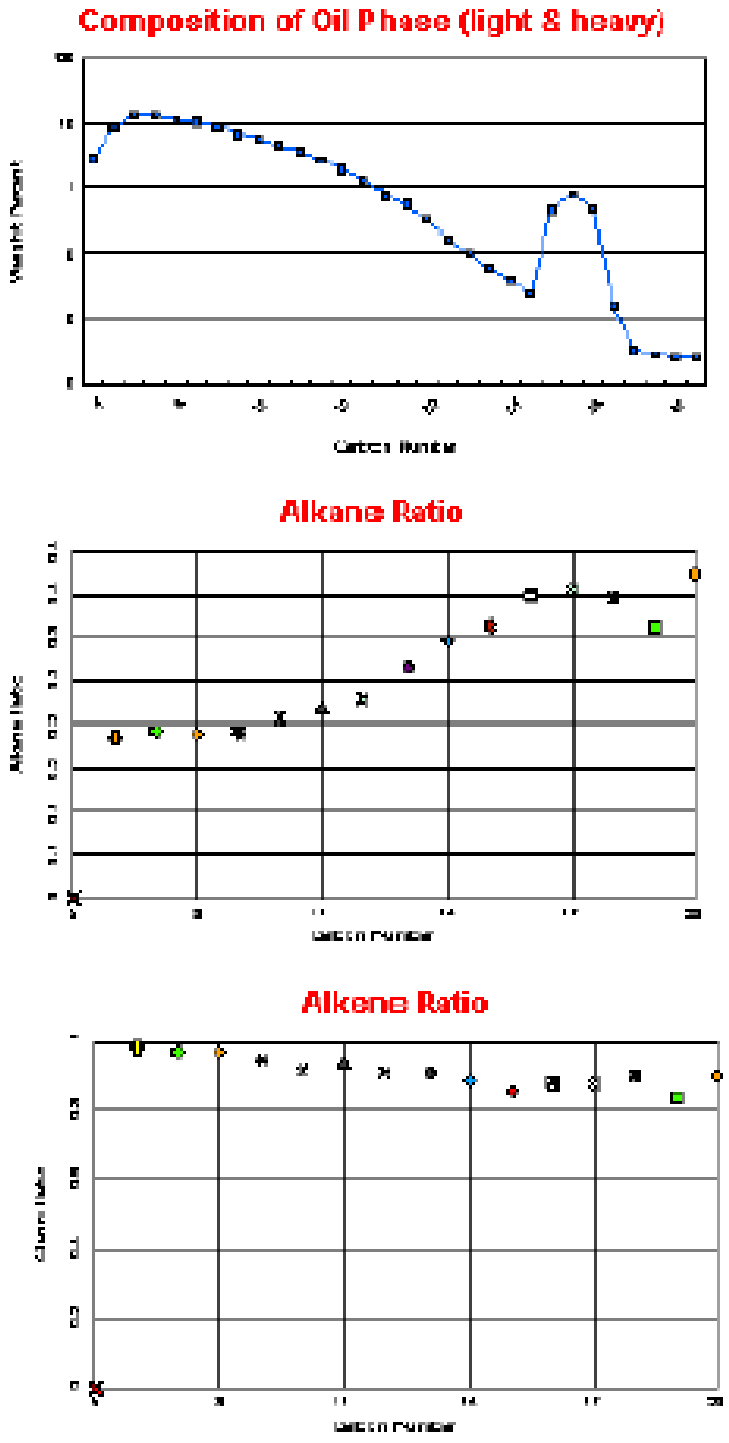

Figure 19. Oil Phase Distribution Binder Silica, CAER data.

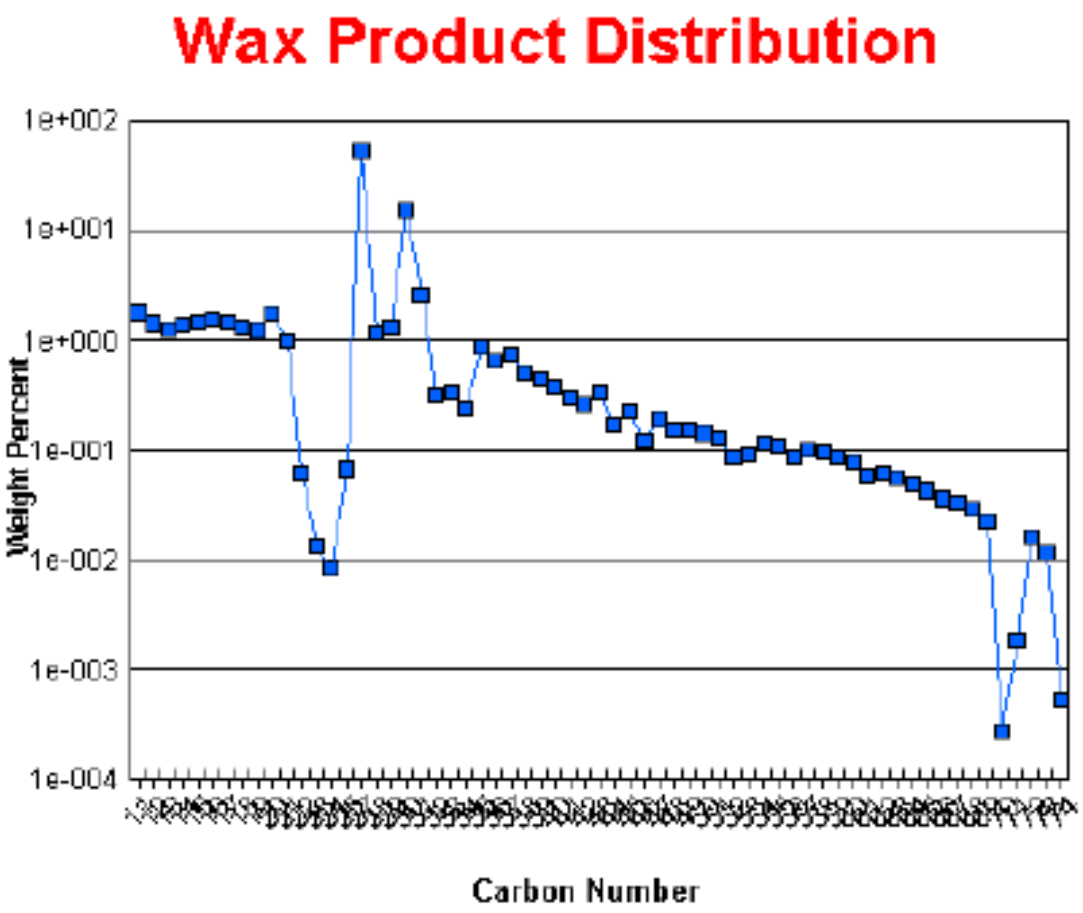

Figure 20. Wax Product Distribution Binder Silica, CAER data.

Literature References

1. Allen, T., *Particle Size Measurement*, 5th ed., Chapman & Hall, New York (1997).

2. Amelse, J.A. butt, J.B., and Schwartz, L.H., J. Phys. Chem., 82, 558(1978).

3. Amelse, J.A., Schwartz, S.T., and Butt, J.B., J. Catal., 87, 179(1984).

4. Anderson, R.B., The Fischer-Tropsch Synthesis; Academic Press: Orlando, FL, 1984.

5. ASTM D-32.02.06, DI Test of Attrition Resistance.

6. Bessel, S., U.S. Patent, 5, 126, 377(1992).

7. Bhatt, B.L., *Liquid Phase Fischer-Tropsch(II) Demonstration* in *"The LaPorte Alternative Fuels Development Unit, Performer: Air Products and Chemicals",* Allentown, PA, PR: PC A07/MF A02

8. Bhatt, B.L., Schaub, E.S., Heydorn, E.C., Herron, D.M., Studer, D.W., Brown, D.M., in "Proc. Of Liquefaction Contractors Review Conference", (G.J. Stiegel and R.D. Srivastava, Eds.), U.S. Department of Energy, Pittsburgh, 1992, p. 403.

9. Bukur, D.B., and Lang, X., Studies in Surface Science and Catalysis, 119, 118 (1998).

10. Bukur, D.B., Carreto-Vazquez, V., Pham, H.N., Datye, A.K. (submitted).

11. Bukur, D.B., Lang, X., *Ind. Eng. Chem. Res*. 38 (1999) 3270.

12. Bukur, D.B., Lang, X., Mukesh, D., Zimmerman, W.H., and Li, C., J. Catal., 29, 1588(1990b).

13. Bukur, D.B., Mukesh, D., and Patel, S.A., Ind. Eng. Chem. Res., 29, 194 (1990a).

14. Bukur, D.B., Nowicki, L., Lang, X., *Chem. Eng. Sci*. 49 (1994) 4615.

15. Bukur, D.B., Nowicki, L., Manne, R.K., and Lang, X., J. Catal., 155, 366(1995b).

16. Bukur, D.B., Okabe, K., Li, C., Wang, D., Rao, K.R.P.M., and Huffman, G.P., J. Catal., 155, 353(1995a).

17. Bukur, D.B., Patel, S., and Lang, X., *App. Catal. A* 61 (1990) 186, 329.

18. Butt, J.B., Catal. Lett., 7, 61(1990).

19. Datye, A.K., and Shroff, M.D., Harrington, M.S., Sault, A.G., and Jackson, N.B., Studies in Surface Science and Catalysis, 107, 169 (1997).

20. Davis, B.H., Zu, L., and Bao, S., Studies in Surface Science and Catalysis,107, 175 (1997).

21. Donnelly, T.J., and Satterfield, C.N., Appl. Catal., 56, 231(1989).
22. Dry, Appl. Catal., 138, 319(1996).

23. Dry, M., in Catalysis: Science and Technology, Vol. 1, ed. By Anderson, J.R., Springer-Verlag, NY, 1981.

24. Gormley, R.J., Zarochak, M.F., and Deffenbaugh, P.W., Appl. Catal. A: General, 161, 263(1997).

25. Jaeger, B., *Studies in Surface Science and Catalysis*, 107, 219 (1997).

26. Jager, B., Espinoza, R., *Catal. Today*, 23 (1995) 17.

27. Jager, B., Van Berge, P., Steynberg, A.P., *Stud. Surf. Sci. Catal*. 136 (2001) 63.

28. Jothimurugesan, K., Goodwin Jr., J.G., Gangwal, S.K., Spivey, J.J., *Catal. Today* 58 (2000) 335.

29. Jothimurugesan, K., Spivey, J.J., Gangwal, S.K., and Goodwin, J.G., Studies in Surface Science and Catalysis, 119, 215 (1998).

30. Jothimurugesan, K., Spivey, J.J., Gangwal, S.K., and Goodwin, Jr., J.G., Development of Fe Fischer-Tropsch Catalysts for Slurry Bubble Column Reactors, ACS meeting, Anaheim, CA, March 21-25, 1999a. Abstract accepted.

31. Jothimurugesan, K., Spivey, J.J., Gangwal, S.K., and Goodwin, Jr., J.G., Development of Fe Fischer-Tropsch Catalysts with High Attrition Resistance, Activity, and Selectivity, Spring AIChE meeting, Houston, TX, March 14-18, 1999b. Abstract accepted.

32. Jothimurugesan, K., Spivey, J.J., Gangwal, S.K., and Goodwin, Jr., J.G., Attrition Resistant Iron-Based Fischer-Tropsch Catalysis, 16th Meeting of the North American Catalysis Society, Boston, MA, May 30-June 4, 1999c. Abstract accepted.

33. Jothimurugesan, K., Spivey, J.J., Gangwal, S.K., Goodwin Jr., J.G., *Stud. Surf. Sci. Catal*. 119 (1998) 215.

34. Kalakkad, D.S., Shroff, M.D., Kohler, S., Jackson, N., Datye, A.K., *Appl. Catal. A* 133 (1995) 335.

35. Kalakkad, D.S., Shroff, M.D., Kohlers, S., Jackson, N., and Datye, A.K., Appl. Catal., 133, 335 (1995).

36. Kolbel, H., and Ralek, M., Catal. Rev.-Sci. Eng., 21, 225(1980).

37. Lang, X., Akgerman, A., and Bukur, D.B., Ind. Eng. Chem. Res., 34, 73(1995).

38. Lee, S.K., Jiang, X., Keener, T.C., and Khang, S.J., Ind. Eng. Chem. Res., 32, 2758 (1993).
39. Milburn, D.R., Komandur, V.R., Chary, V.R., O'Brien, R.J., and Davis, B.H., Appl. Catal., 144, 133 (1996).

40. O'Brien, R.J., Raje, A., Keogh, R.A., Spicer, R.L., Xu, L., Bao, S., Srinivasan, R., Houpt, D.J., Chokkram, S., and Davis, B.H., Coal Liquefaction and Gas Conversion Contractors' Review Conference, 1995.

41. O'Brien, R.J., Xu, L., Bao, S., Raje, A., Davis, B.H., *Appl. Catal. A* 196 (2000) 173.

42. Pennline, H.W., Zarochak, M.F., Stencel, J.M., and Diehl, J.R., Ind. Eng. Chem. Res., 26, 595 (1987).

43. Pham, H.N., Datye, A.K., *Catal. Today* 58 (2000) 233.

44. Pham, H.N., Nowicki, L., Xu, J., Datye, A.K., Bukur, D.B., C. Bartholomew, *Ind. Eng. Chem. Res*. (in press).

45. Pham, H.N., Reardon, J., Datye, A.K., *Powder Technol*. 103 (1999) 95.

46. Pham, H.N., Viergutz, A., Gormley, R.J., Datye, A.K., *Powder Technol*. 110 (2000) 196.

47. Rao, V.U.S., Stiegel, G.J., Cinquegrane, G.J., and Srivastava, R.D., Fuel Proc. Technology, 30, 83 (1992).

48. *Satterfield,* Heterogeneous Catalysis in Practice*, 1991*.

49. Sault, A.G., and Datye, A.K., J. Catal., 140, 136(1993).

50. Shroff, M.D., Kalakkad, D.s., Coulter, K.E., Sault, A.G., and Datye, A.K., J. Catal., 156, 185 (1995).

51. Singleton and Regier, Hydrocarbon Processing, 62, 71 (1983).

52. Soled, G., Iglesia, E., and Fiato, R.A., Catal. Lett., 7, 271 (1990).

53. Srinivasan, R., Xu, L., Spiver, R.L., Tungate, F.L., Davis, B.H., Fuel *Sci. Technol. Int*. 14 (1996) 1337.

54. Srivastava, R.D., McIlvried, H.G., Winslow, J.C., Venktaraman, V.K., and Driscoll, D.J., "Proceedings of the FiF-Teenth Annual International Pittsburgh Coal Conference", Pittsburgh, PA, September 14, 1998.

55. Srivastava, R.D., Rao, V.U.S., Cinquegrane, G., and Stiegel, G.J., Hydrocarbon Processing, 1990.

56. Stiles, A.B., Catalyst Manufacture, Marcel Dekker, Inc., New York, 1983.
57. Sudsakorn, K., Goodwin Jr., J.G., Jothimurugesan, K., Adeyiga, A.A., *Ind. Eng. Chem. Res*., 40 (2001) 4778.

58. Ward, A.D., and Ko, E.I., Ind. Eng. Chem. Res., 34, 421 (1995).

59. Wei, D., Goodwin Jr., J.G., Oukaci, R., Singleton, A.H., *Appl. Catal*. A 210 (2001) 137.

60. Zarochak, M.F., and McDonald, M.A., in Seventh DOE Indirect Liquefaction Contractors Meet Proc., Pittsburgh, Dec. 7-9, p. 96 (1987).

61. Zhao, R., Goodwin Jr., J.G., Jothimurugesan, K., Gangwal, S.K., Spivey, J.J., *Ind. Eng. Chem. Res*. 40 (2001) 1065.

62. Zhao, R., Goodwin Jr., J.G., Jothimurugesan, K., Gangwal, S.K., Spivey, J.J., *Ind. Eng. Chem. Res*. 40 (2001) 1320.

63. Zhao, R., Goodwin Jr., J.G., Oukaci, R., *Appl. Catal. A* 189 (1999) 99.

64. Zhao, R., Sudsakorn, K., Goodwin Jr., J.G., Jothimurugesan, K., Ganwal, S.K., Spivey, J.J., Spivey, J.J., *Cat. Today*, 71 (2002) 319.

65. Zhao, R., Sudsakorn, K., Goodwin Jr., J.G., Jothimurugesan, K. Spivey, J.J., and Gangwal, S.K., *Ins. Eng. Chem. Res.* 39, 1155 (2000).

APPENDIX A:
ATTRITION INDEX CALCULATIONS

Weight Percentage of Fines Lost

"Weight percentage of fines lost" was basically the percentage ratio of the weight of fines (W_f) collected by thimble, installed at the jet cup exit, and the weight of the total particles recovered (W_r) in the jet cup at the end of an attrition test:

W_r = weight of fines generated (W_f)

+ weight of particles remaining at the bottom (W_b) **(A-1)**

$$\text{Weight percentage of fines lost (\%)} = \frac{W_f}{W_r} \times 100 \quad \textbf{(A-2)}$$

Net Change in Volume Moment

"Net change in volume moment" was the percentage ratio of the difference of volume moments (X_{VM}) before and aF-Ter attrition test and the volume moment before attrition test:

$$\text{Net change in volume moment (\%)} = \frac{\left(X_{VM}, before\ attrition - X_{VM}, after\ attrition\right)}{X_{VM}, before\ attrition} \times 100 \quad \textbf{(A3)}$$

$$\text{Volume moment } (X_{VM}) = \frac{\sum X^4 dN}{\sum X^3 dN} \quad \textbf{(A-4)}$$

Where N is the number of particles of size X.

APPENDIX B:
FE REDUCIBILITY CALCULATION

The Fe reducibility by H_2 TPR was calculated based on the following assumptions:

Assumption: 1) all Fe in a calcined Fe catalyst is in form of Fe_2O_3.

2) all Cu and K in the catalyst are in the form of CuO and K_2O, respectively.

3) Fe_2O_3 reacts with H_2 as: $Fe_2O_3 + 3\ H_2 = 2\ Fe + 3\ H_2O$. (B-1)

Example: Calculation of Fe reducibility for 100 Fe/5Cu/4.2K/21SiO_2

100 g or (100/55.8 = 1.8 mol) of Fe comes from (1.8/2 mol or 143.6 g of Fe_2O_3)

5 g or (5/63.5 = 0.08 mol) of Cu comes from 0.08 mol or 6.4 g of CuO)

4.2 g or 4.2/39.1 = 0.11 mol) of K comes from (0.08/2 mol or 10.4 g of K_2O)

The weight of these components added to 21 g of SiO_2 gives the total catalyst weight of:

Total catalyst wt. = 143.6 + 6.4 + 10.4 + 21 = 181.4 g.

Therefore, 1 g total calcined catalyst weight contains:

100/(55.8 * 181.4) = 0.01 mol of Fe or 143.6/(159.6 * 181.4) = 0.005 mol of Fe_2O_3

$5/(63.5 * 181.4) = 4.3 * 10^{-4}$ mol of Cu

$4.2/(39.1 * 181.4) = 5.9 * 10^{-4}$ mol of K and

$21/(60.1 * 181.4) = 5.5 * 10^{-3}$ mol of SiO_2.

From equation (B-1) mol Fe_2O_3 consumes 3 * 0.005 = <u>0.015 mol H_2/g-cat</u>. This amount of H_2 consumed represents 100% of Fe reducibility. The Fe reducibilities reported are the percentages of this amount.